LIFE PREDICTION OF SPOT-WELDS
A Fatigue Crack Growth Approach

by

John Andrew Newman

Thesis submitted to the Faculty of the
Virginia Polytechnic Institute and State University
in partial fulfillment of the requirement for the degree of

MASTER OF SCIENCE
in
Engineering Mechanics

APPROVED:

N. E. Dowling

J. C. Duke

R.W. Landgraf

DECEMBER, 1996
BLACKSBURG, VIRGINIA

Keywords: Spot-welds, fatigue, crack growth, life prediction, stress intensity factors, Walker equation

LIFE PREDICTION OF SPOT-WELDS
A Fatigue Crack Growth Approach

by

John Andrew Newman

Dr. Norman E. Dowling, Chairman

Engineering Science and Mechanics

(ABSTRACT)

A life prediction method is developed for spot-welds subject to fatigue loading. Stress intensity factors are used with the Walker equation to develop two crack growth approaches to the problem. The predictions fit data for lap joint configurations well, but not so for peel joint geometries.

TABLE OF CONTENTS

ACKNOWLEDGMENTS

I wish to thank Ford Motor Company for providing funds and specimens that made this project possible. Yuting Rui, the technical advisor from Ford has provided valuable input over the many months this project was in full swing. My advisor here at Virginia Tech, Dr. Norman Dowling, deserves my thanks the most for putting up with me on a weekly and sometimes daily basis. His guidance was helpful and greatly needed. I am lucky to know Dr. Dowling. Dr. J. C. Duke and Dr. R. W. Landgraf have also been a great help over the past few months. Bob Simonds, Mac McCord, and George Lough have provided needed technical support and instruction in operating lab equipment. Brian Gero, a fellow student working on this project has been a great help in running and (yawn) watching fatigue tests at all hours of the day and night. Russ Chernenkoff at Ford Motor Company was nice enough to make an attempt to find good Walker equation constants for weld metal.

This is dedicated to my late grandmother, Lila Bolt Newman (1903-1995), who died while this work was in progress. From humble roots in Carroll County, Virginia, she worked hard to improve life for herself, her four daughters, and one son (my father). Amazingly, she afforded my father the luxury of a college education so his life would be better than hers. I hope she knows how the lives of her family members have been greatly improved by her efforts.

LIST OF VARIABLES WITH DESCRIPTIONS

A	constant used in several equations
a_i	initial crack length
a_f	final crack length
$\underline{a}$	constant used in Peterson's equation
B	constant
b	constant used in the Basquin relation
C	constant used in Paris power law, Walker's equation, and other equations
D	spot-weld diameter, assuming a circular weld, constant in some equations
E	elastic modulus
ΔE	damage parameter
F	force
F_1	force in the x_1 - direction
F_2	force in the x_2 - direction
F_3	force in the x_3 - direction
G	total strain energy release rate
G_I	strain energy release rate due to a mode I stress intensity
G_{II}	strain energy release rate due to a mode II stress intensity
G_{III}	strain energy release rate due to a mode III stress intensity
H	dummy constant used to group several constants together
K_f	fatigue notch factor
K_f^{max}	extreme value of K_f
K_{MIN}	minimum stress intensity factor
K_{MAX}	maximum stress intensity factor
K_t	elastic stress concentration factor

K_I	opening mode stress intensity factor (mode I)
K_{II}	sliding mode stress intensity factor (mode II)
K_{III}	tearing mode stress intensity factor (mode III)
ΔK	range of stress intensity factors
K_I^{eff}	effective mode I stress intensity factor used in mixed mode situations
ΔK_I^{eff}	range of K_I^{eff}
L	constant used in Sec. 2.2
M_1	moment in the x_1 - direction
M_2	moment in the x_2 - direction
M_3	moment in the x_3 - direction
m	constant used in Walker's equation
N	specimen life
N_i	portion of life devoted to creating a crack of length a_i
N_f	life of specimen to some degree of failure
N_I	portion of specimen life spent creating a crack, also cycles to crack initiation used in the Basquin relation
N_{II}	portion of life spent growing a crack through one or more sheets of metal
N_{III}	portion of life remaining after the first two stages of life
n	constant used in Paris power law and other equations
ΔP	range of loading
$\overline{P^{max}}$	effective zero-to-max load
Q	constant used in Sec. 2.2
R	load ratio, also used as stress intensity ratio
r	radial coordinate used in the vicinity of the crack tip, weld radius
ΔS	range of remotely applied stress
t	thickness of sheet metal

α	constant used in formula for K_t of a tensile-shear spot-weld
β	constant relating the contribution of K_{II} to K_I^{eff}
$\Delta\varepsilon$	range of strain, locally
ϕ	angle in the weld plane measured from the x_1 axis in the x_2 direction
γ	constant used in Walker's equation
σ_a	local stress amplitude
σ_f'	material constant used in Basquin relation
σ_m	mean stress
σ_r	radial stress near the crack tip for a two-dimensional crack
σ_{rr}	radial stress near the crack tip for a two-dimensional crack (different formulation)
σ_Θ	tangential stress near the crack tip for a two-dimensional crack
$\sigma_{\Theta\Theta}$	tangential stress near the crack tip for a two-dimensional crack (different formulation)
$\Delta\sigma$	range of stress locally
ν	Poison's ratio
θ	angular coordinate used in the vicinity of the crack tip
Θ_o	a specific value of Θ chosen as the direction of crack growth
$\Delta\Theta$	range of weld rotation
$\Delta\Theta_N$	range of weld rotation, measured from the normal or x_3-axis
$\tau_{r\Theta}$	in-plane shear stress near the vicinity of the crack tip

1. INTRODUCTION

In this chapter, the topic of spot weld fatigue is introduced. Why this topic is important, the nature of this project, and work previously done on the topic of spot weld fatigue are discussed.

1.1 Motivation

Why is understanding spot-weld fatigue important? It is important because spot-welding is a commonly used method of joining sheets of metals. Although spot-welds have been used for many years, predicting exactly what occurs in and around the weld is very difficult and has eluded previous researchers. Complex geometries, a non-homogeneous metallurgical structure, and residual stresses make analysis extremely difficult. It is the purpose of this project to develop a life prediction method for spot-welded metals. Understanding fatigue performance of spot-welds is important when designing a spot-welded structure.

1.2 Project Details

This study of spot-weld fatigue is sponsored by Ford Motor Company, which has provided funds and specimens in order for this research to take place. Two categories of specimens have been provided. The simplest specimens are called coupons, consist of two strips of sheet steel connected by a single spot-weld and come in two types, lap joints and peel joints. The second category of specimen is a structure which consists of more than two pieces of sheet steel connected by multiple welds. Only one type of structure specimen was provided, box joints. Specimens are constructed of two types of steel, those being SAE 1010 steel (mild steel) and SAE 950X steel (high-strength steel). Ford

is concerned with the performance of these spot-welded metals and their application to automobiles. It is hoped that simpler geometries found in coupon specimens will help develop understanding of what is occurring in a spot-welded structure.

1.3 Literature Review

Spot-welding is the most common way to join sheets of steel or other metal alloys for automotive applications. Although spot-welds are common, studying and predicting their behavior is complicated by residual stresses created from the welding process, complex stresses around the weld, and, in some cases, large deflections around welds. In recent years, automotive manufacturers have started using thinner sheets of higher strength steels in place of thicker low-strength steels. Although reducing the weight of automobiles and other structures is a good cause, it must be done carefully because high-strength steels tend to hold no advantage under fatigue loading.[1] High strength steels are superior when no cracks are present, but this is not the case for spot-welds.[2] Weld performance under static loading is used to judge weld quality, although such information has almost no use in a fatigue analysis.[3] Furthermore, the deflections associated with static rupture of a spot-welded joint are well beyond acceptable limits for most applications.[4] The use of thinner high strength steel sheets joined by spot-welds seems to have spurred interest in analyzing and predicting the fatigue performance of these connections, although many researchers do not agree on the mechanisms that cause failure.

Some researchers, including F. V. Lawrence and many of his graduate students, believe the spot-weld connection has a finite radius and thus behaves as a notch. [5,6,7,8] The initiation of a crack-like defect would, in this case, be a separate and distinguishable event from crack propagation. Other researchers, including S. D. Sheppard and J. F. Cooper, believe that spot-welds initially behave as a crack and propagation begins from

the first cycle of loading. [9,10,11,12] There are researchers that use structural stresses to predict fatigue behavior. [13,14,4,15] This method entails converting the applied load into a stress by using the cross-sectional area of the steel strip, or the area of the weld. This structural (or average) stress is then plotted against the cycles to failure (for constant amplitude loading) to obtain an appropriate relation from data empirically. The two types of approaches that consume the attention of most of the literature are notch approaches, supported largely by F. V. Lawrence, and crack growth approaches, supported by S. D. Sheppard, J. F. Cooper, and numerous others.

1.3.1 The Welding Process

Electrical resistance spot-welding uses large amounts of alternating electrical current to heat and melt a region around two or more sheets of metal. Upon cooling the melted region solidifies into one solid lump joining the once separate metal sheets. Top and bottom electrodes are forced against the sheets to ensure contact to complete an electrical circuit between electrodes. The variables involved, electrode force, current, hold time, and cycles of current allowed into the weld, etc., to produce a sound spot-weld are known but not universally accepted as to their specific values. Much work has been performed to investigate the effects of these variables on weld performance for static, fatigue, and impact cases. Most of the concern about the welding process deals with producing a sufficiently large weld diameter and the effects of welding heat on the metal surrounding the weld. [16,8,17]

1.3.2 Failure Modes

Failure in a spot-weld occurs in the heat affected zone (HAZ) of unmelted metal between the base metal and the weld metal. The HAZ is caused by the extreme heat of welding

changing metallurgical properties on the microscopic level. The HAZ is subjected to higher stresses than the surrounding base metal and is the location of failure in most cases. Work has been done to examine damage to the HAZ subjected to low-cycle fatigue and continuum damage mechanics (CDM) has been used to model accumulating damage in this region. [18,19,20] CDM models are developed to describe damage on the microscopic level and only for high stress levels associated with low cycle fatigue. Microscopic properties of the base metal, such as grain size, have been found to have no effect on high cycle fatigue of its HAZ.[21] Residual stresses, which are associated with the HAZ, can significantly alter fatigue lives. [11] For this reason alone, the HAZ should be considered as a distinct region separate from the surrounding base metal.

A well made spot-weld should not fail across its weld metal. Failure of the weld metal seems to be associated with yielding by shear. If the weld does not fail by yielding, fatigue crack growth in this region does not occur.[1] The weld metal seems to have material and fatigue properties superior to the surrounding base metal. A weld is very nearly circular and is characterized with a diameter, D. In order to produce welds that won't fail by gross yielding of weld metal, a spot-weld needs to satisfy Eq. 1.1. [22]

$$D \geq \sqrt{t} \qquad \text{(D and t in inches)} \qquad (1.1\text{-a})$$

$$D \geq 5\sqrt{t} \qquad \text{(D and t in mm)} \qquad (1.1\text{-b})$$

where t is the sheet thickness.

Failures of spot-welds can be placed into several categories. First of all, if a weld nugget is too small, or if too little current was used during welding, failure by yielding across the nugget may occur. [2] Such a failure would be considered to be caused by poor welding. In most cases, however, cracks would lead to failure where the stress intensity factors are greatest. [23] This crack propagates from the edge of the weld metal into the HAZ. Once a crack develops, one of two things may happen. If the load is sufficiently small, the

crack will propagate far from the weld into the base metal before plastic instability ruptures the specimen. However, if the load is sufficiently high, the crack is not allowed to grow far before plastic effects tear the crack around the weld. [8] This makes the crack appear to have an eyebrow (curved) shape. [24] The greater the loads the more the crack curves around the weld. Sometimes the weld may pull out of one of the sheets like a can tab is pulled out of the top of a can.

Spot-welded specimens come in many different types. Coupon specimens usually consist of a single spot-weld connecting two pieces of sheet metal. Some coupons consist of multiple welds, but still connect only two pieces of sheet metal. More complicated specimens are lumped into the category of structures, which consist of multiple welds and more than two pieces of sheet metal. [25, 27] Multiple welds introduce greater difficulty in analysis because the stress distributions around welds may interact. The most common coupon specimen has a lap-shear geometry. Two strips of metal are laid such that the ends overlap and one or more welds connect these strips. The specimen is then loaded such that a shear condition occurs across the weld. Other geometries exist, which create a variety of loading conditions, but the lap-shear geometry is one of the strongest and most common geometries used.

1.3.3 Notch analysis

Researchers who consider the spot-weld connection to behave as a notch, divide the life (of a spot-weld) into three distinct stages. The first stage is spent initiating a crack from a notch-like connection. The second stage is governed by fatigue crack growth from the connection at the interface of the two sheets completely through one steel sheet to the outside. In the third stage of life, the crack propagates away from the spot-weld, grows into the surrounding base metal, and ends when the specimen is in two or more separate pieces. The number of cycles for the first stage is N_I, while the life for the second and

third stages are N_{II} and N_{III} respectively. Thus, the total life of the specimen, N is the sum of the lives of the three stages[25, 26]

$$N = N_I + N_{II} + N_{III} \tag{1.2}$$

Each stage of spot-weld life is modeled separately because each stage is governed by a different mechanism of damage accumulation. The first stage is typically analyzed by a strain-based approach. Some work has been done experimentally using strain gages on the outer face of a specimen and relating that strain to the strain at the notch. [27, 28] The remote stress is related to the local stress and strain found at the notch by [29]

$$\Delta\sigma \cdot \Delta\varepsilon = \frac{(K_f \Delta S)^2}{E} \tag{1.3}$$

where E is the elastic modulus, ΔS is the remote applied stress, $\Delta\sigma$ is the local stress at the notch, $\Delta\varepsilon$ is the local strain at the notch, and K_f is the fatigue notch factor appropriate for the notch geometry. [5]

In order to find the fatigue notch factor, K_f, the elastic stress concentration factor, K_t, is needed. An estimate for K_t obtained by a finite element scheme[6] for a tensile-shear spot-weld geometry is given by,

$$K_t = 1 + \alpha\left(\frac{t}{r}\right)^{1/2} \tag{1.4}$$

where the notch radius is r and α is a material constant. [29] Then, K_f is usually estimated using Peterson's equation,

$$K_f = 1 + \frac{K_t - 1}{1 + \frac{\underline{a}}{r}} \tag{1.5}$$

where r is the notch radius and $\underline{a}$ is another material constant. [29] The actual notch radius of a spot-weld connection is not very well defined. It is assumed that the radius has no specific value, so the worst possible value for a notch radius is used. Extrema for K_f can

be found by finding where its derivative with respect to the notch radius, r, goes to zero. This is a maximum and is given as K_f^{max}. [29]

$$K_f^{max} = 1 + \frac{\alpha}{2}\left(\frac{t}{a}\right)^{1/2} \tag{1.6}$$

The initiation life is estimated by modifying the empirical Basquin relationship with the Morrow mean stress correction, which is given as follows. [25]

$$\sigma_a = \left(\sigma_f' - \sigma_m\right)\left[2N_I\right]^b \tag{1.7}$$

where N_I is the number of cycles to crack initiation, σ_a is the local stress amplitude, σ_m is the mean stress, and σ_f' and b are material constants.

The Basquin relationship is modified by expressing the stress amplitude in terms of applied stress and the fatigue notch factor, K_f. The modified Basquin relationship is, [25]

$$\frac{\Delta S}{2}K_f = \left[\sigma_f' - \sigma_m\right]\left(2N_I\right)^b \tag{1.8}$$

Choosing the constants for this empirical equation may be troublesome. Some effort should be made to obtain the constants for the heat affected zone (HAZ), which is where cracks are found. Furthermore, Peterson's equation (Eq. 1.5) may not be valid for an arbitrarily small notch radius.[30] Peterson himself warned that his equation was only intended for machined notches with a finite radius whose depth was not much greater that the notch radius. [31] As a notch becomes smaller, the fatigue notch factor, K_f, should increase because the notch is approaching the geometry of a sharp crack. It seems unreasonable to expect a vanishingly small notch radius to produce a longer life than a larger notch radius for the same loading conditions.

All researchers agree that there exists a portion of spot-weld life devoted to propagating a crack through the thickness of one or both sheets. Those that believe a notch exists initially state that up to 50% of the total life, N_T, is spent initiating a crack. [5] Naturally,

this percentage is dependent upon maximum load and the load ratio, R, for constant amplitude loading. An arbitrarily small crack length, a_i, is chosen to determine the end of the first stage. The ability to detect a crack determines this initial crack size. Lawrence and other workers have chosen to consider a crack length of 0.25 mm to be their initial crack length. [5, 32] Considering that a typical spot-weld joins sheet metal on the order of 1mm thick, this initial crack size is not a negligible portion of the total thickness. Sheppard and Strange pointed out that at a life of one million (10^6) cycles, a crack was detected after 30% of a specimen life had passed. For this particular case, the crack was already 20% through the sheet metal thickness. [9] It seems unreasonable to partition the first 30% of life from the last 70% given these numbers.

1.3.4 Fatigue Crack Growth Analysis

As previously stated, all researches agree that fatigue crack growth is responsible for at least a portion of the life of spot-welded joints. The majority believe that a crack-like defect exists at the spot-weld connection initially and crack growth begins on the first cycle. In this case the initiation life, N_I, would not exist or at least represent a negligible portion of the total life. Exactly what takes place is somewhat of a mystery because the spot-weld connection is not accessible for observation. Destructive tests performed on specimens interrupted before failure support the claims of a crack present at an early stage in the weld life. [9, 13] Nondestructive tests, such as the electric potential drop method, also tend to indicate that early crack growth is a reality. [10, 33] The electric potential drop method detects the presence of a crack by passing a direct electrical current through a region in which a crack is expected to form. The presence of the crack increases the electrical resistance, which in turn decreases the voltage (potential), measured across the weld. [32]

Most workers that try to quantify crack extension use a form of the Paris power law which is of the following form. [34, 35, 36, 37, 38]

$$\frac{da}{dN} = C(\Delta K)^n \tag{1.9}$$

where C and n are material constants (where C is also dependent upon the load ratio, R). The crack length is represented by "a" and the number of cycles is N. ΔK is an appropriate stress intensity factor as will be discussed later.

1.3.5 Mixed Mode Behavior

The Paris power law requires knowledge of an equivalent Mode I stress intensity factor. In general, the loading of a spot-weld induces all three modes of stress intensities. Each

of the three stress intensity factors promote damage, but because a crack tends to propagate in the direction that maximizes K_I, the Paris power law is expressed using a mode I stress intensity factor. [39, 40, 41] Modes II and III tend to steer a crack in the direction of maximum K_I, which hastens crack growth. [42] Some workers suggest use of energy release rates of crack extension, G, instead of stress intensities. Attempts to quantify stresses at a crack tip using elastic stress solutions may not be useful due to the presence of a plastic zone. [41] The strain energy release rate has another advantage in that its effects can be summed for each of the three modes as follows.

$$G = G_I + G_{II} + G_{III} \tag{1.10}$$

Because the strain energy release rate is proportional to the square of the stress intensity factor for its corresponding mode, this indicates that an elliptical relation exists between K, K_I, K_{II}, and K_{III}, where K is the effective mode I stress intensity factor used in the Paris power law (Eq. 1.9). Possible formulations for K are given below. [14, 39]

$$K = \sqrt{K_I^{\,2} + \beta \cdot K_{II}^{\,2}} \qquad \text{(for Modes I and II only)} \tag{1.11-a}$$

$$K = \left[K_I^{\,4} + 8 K_{II}^{\,4} + \frac{8 K_{III}^{\,4}}{1-\nu} \right]^{1/4} \tag{1.11-b}$$

where ν is Poison's ratio and β is a material constant.

Work has been done, by G. C Sih and others, to examine the behavior of mixed mode fatigue behavior. [41] Studies of modes I and II acting on cracks in brittle materials indicates that a crack propagates perpendicular to the maximum tensile normal stress. For a crack subject to modes I and II of crack opening, the in-plane stresses at the crack tip expressed in polar coordinates are given as Eqs. 1.12 a-c. [41]

$$\sigma_r = \frac{1}{\sqrt{2\pi\, r}} \cos\frac{\Theta}{2} \left[K_I \left(1 + \sin^2 \frac{\Theta}{2} \right) + \frac{3}{2} K_{II} \sin\Theta - 2 K_{II} \tan\frac{\Theta}{2} \right] \tag{1.12-a}$$

$$\sigma_{\Theta} = \frac{1}{\sqrt{2\pi\, r}} \cos\frac{\Theta}{2}\left[K_I \cos^2\frac{\Theta}{2} - K_{II}\sin\Theta \right] \qquad (1.12\text{-b})$$

$$\tau_{r\Theta} = \frac{1}{2\sqrt{2\pi\, r}} \cos\frac{\Theta}{2}\left(K_I \sin\Theta + K_{II}(3\cos\Theta - 1) \right) \qquad (1.12\text{-c})$$

Since the crack is assumed to grow along principal stress planes, the angle of crack propagation is that which causes the in-plane shear stress to equal zero. Thus, the angle of initial crack propagation satisfies the following relation. [23]

$$K_I \sin\Theta = -K_{II}(3\cos\Theta - 1) \qquad (1.13)$$

A crack grows perpendicular to the maximum tensile normal stress for perfectly brittle materials. Most metals, such as steel, also tend to follow this trend. These materials have small crack tip plastic zones and a change in crack direction from a mixed mode configuration to one of pure Mode I occurs almost instantly such that the crack changes direction at a kink. A ductile material such as low strength steel displays similar behavior with the possible exception of the sudden change in crack direction indicated by a kink. For steels, and most metals, Modes II and III would probably take longer (a greater percentage of life) to re-orient a crack such that K_I is maximized. [42] The size of the plastic zone may be some measure of the "turning radius" of a mixed mode crack subject to fatigue loading.

1.3.6 Stress Intensity Factors

Stress Intensity Factors for Half-Subspaces Connected by a Circular Neck

A possible first model of a spot-weld is that of two half-spaces connected by a circular or elliptical neck. For this paper, only circular welds are considered so that radial symmetry may be assumed where needed. A half-space is a semi-infinite body bounded only to one side of an infinite plane. In this crude model, two of these half-spaces share a common boundary plane, but are not connected with the exception of one perfect circle of radius, a. The crack is thus in the boundary plane shared by both half-spaces. The half-spaces are assumed not to interact with one another, such that no compression can take place between them in any region. A coordinate system is established such that the plane of the crack is the x_1-x_2 plane and the coordinate x_3 is perpendicular to the crack plane. In general three forces, F_1, F_2, and F_3, and three moments, M_1, M_2, and M_3, may act on the circular neck. These force and moments generate all three modes of stress intensities. If an angle ϕ is defined as the angle from the x_1 axis in the direction of the x_2 axis, the stress intensity factors on the edge of the neck (radius r) are given in Eqs. 1.14 a-c. The forces, F_i, and moments, M_i, that act on a spot-weld under generalized loading are diagrammed in Figure 1.1.

$$K_I = \frac{1}{2r\sqrt{\pi r}}\left[F_3 + \frac{3M_1\sin\phi}{r} - \frac{3M_2\cos\phi}{r}\right] \tag{1.14.a}$$

$$K_{II} = \frac{1}{2r\sqrt{\pi r}}\left(F_1\cos\phi + F_2\sin\phi\right) \tag{1.14.b}$$

$$K_{III} = \frac{1}{2r\sqrt{\pi r}}\left[F_1\sin\phi + F_2\cos\phi + \frac{3M_3}{2r}\right] \tag{1.14.c}$$

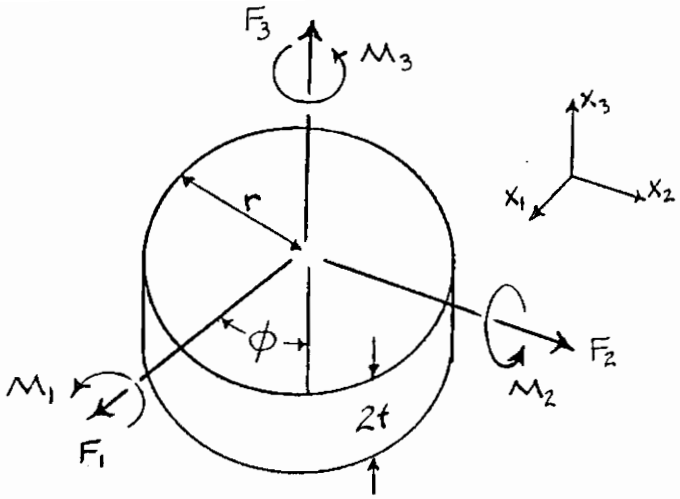

Figure 1.1. Generalized loading on a spot-weld nugget.

Stress Intensity Factors for Finite Geometries Connected by a Circular Neck

The finite dimensions of a spot-welded specimen alter the stress intensity factors from the semi-infinite case significantly. It has been found that the finite width has a negligible effect as long as the specimen is as wide as five spot-weld radii. The finite thickness of the sheet metal has the greatest effect on the stress intensity factors. L. P. Pook[23] has worked out the solutions for the stress intensity factors of a finite body for the purpose of analyzing spot-weld performance. Although his work deals strictly with lap joint geometries and assumes that only one shear force acts on the weld, the methods he uses can be generalized for any geometry or any loading scenario. Assuming that the specimen is sufficiently wide, the stress intensity factors are approximately known and given in Eq. 1.15 a-c. Normal forces, bending moments, and torsion are assumed to contribute as the would for a half-subspace. Since no numerical work was found that analyzed these loadings for a finite body this assumption is necessary.

$$K_I = \frac{1}{r^{3/2}}\left[0.341\left(\frac{2r}{t}\right)^{0.397}\right]\left(F_1\cos\phi + F_2\sin\phi\right) + (0.282)\frac{F_3}{r^{3/2}}$$

$$+(0.846)\frac{M_1\sin\phi}{r^{5/2}} - (0.846)\frac{M_2\sin\phi}{r^{5/2}} \qquad (1.15.a)$$

$$K_{II} = \frac{F_1\cos\phi}{r^{3/2}}\left[0.282 + 0.162\left(\frac{2r}{t}\right)^{0.710}\right] + \frac{F_2\sin\phi}{r^{3/2}}\left[0.282 + 0.162\left(\frac{2r}{t}\right)^{0.710}\right] \qquad (1.15.b)$$

$$K_{III} = \frac{F_1\sin\phi}{r^{3/2}}\left[0.282 + 0.162\left(\frac{2r}{t}\right)^{0.710}\right] + \frac{F_2\cos\phi}{r^{3/2}}\left[0.282 + 0.162\left(\frac{2r}{t}\right)^{0.710}\right]$$

$$+(0.423)\frac{M_3}{r^{5/2}} \qquad (1.15.c)$$

From Eqs. 1.15 a-c, it can be seen that only the shear forces, F_1 and F_2, need to have a thickness correction. As long as the average stress on a weld is less than 80% of the yield stress, the other forces and moments are assumed to need no corrections. In order to calculate the range of stress intensity factors, simply insert the range of forces or moments where static forces and moments are in Eqs. 1.15 a-c. The maximum K_I and K_{II} occur at point A in Figure 1.2, when $\phi = 0$. The maximum K_{III} is found when $\phi = \pm\pi/2$ at point C. The range in stress intensity factors is defined by,

$$\Delta K = K_{MAX} - K_{MIN} \qquad (1.16)$$

ASSUMPTIONS MADE BY L. P. POOK

- Average stress on weld nugget does not exceed 80% of the yield stress.
- Weld nugget has a circular shape.
- Stress intensity factors are given for a point on the outermost circle on the weld (radius, r) and is described by an angle, ϕ, referenced from the x_1 axis.
- Torsion, bending, and normal forces are not altered by finite thickness.
- Specimen is sufficiently wide so that width effects are negligible.

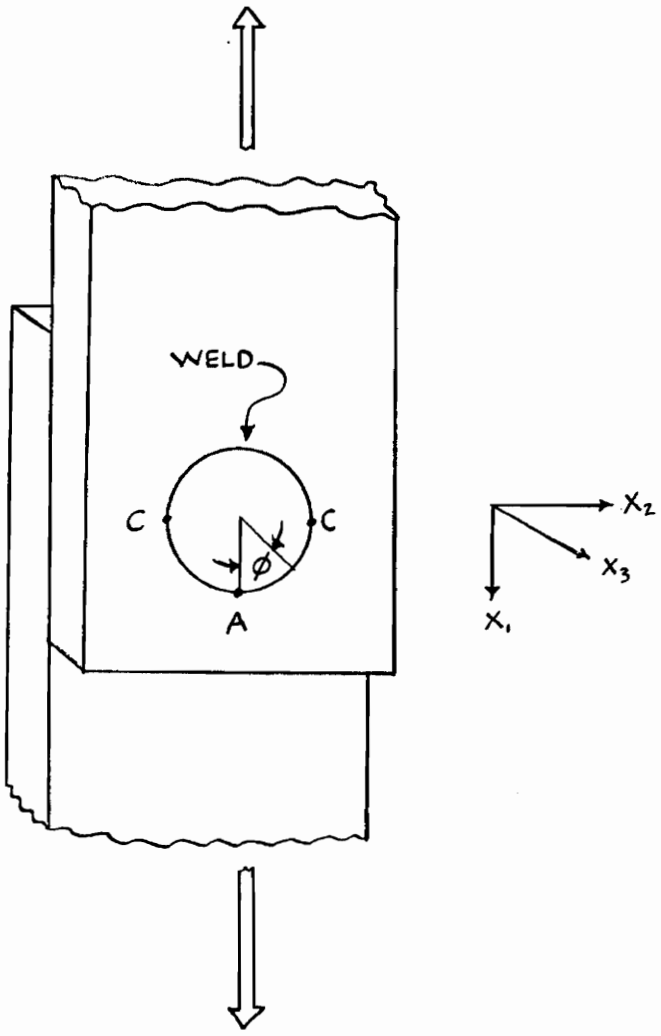

Figure 1.2. Locations of maximum stress intensity factors.
Point A is location of maximum K_I.
Points C are locations of maximum K_{II}

1.3.7 Alternative Representations

Some workers, such as J. L. Overbeeke[43], do not attempt to examine a damage mechanism, as in crack growth or notch initiation. Variables used to predict fatigue performance are fitted to curves empirically. One such method involved examination of the weld nugget rotation. In a lap-shear spot weld specimen, the nugget rotation was found to be proportional to the stress intensity factor squared, which can be expressed symbolically as, [21]

$$\Delta\Theta \propto \left(\Delta K_{EFF}\right)^2 \tag{1.17}$$

This $\Delta\Theta$ was found to be a good indication of fatigue performance. The weld rotation was caused by a small moment created because lap joint specimens are not symmetric.

A damage parameter, ΔE, has been defined for the lap-shear geometry as, [23, 29]

$$\Delta E = \frac{\Delta P \sqrt{\Delta\Theta_N}}{t} \tag{1.18}$$

where $\Delta\Theta_N$ is the range of rotation in the line normal to the spot-weld, ΔP is the change in loading, and t is the sheet thickness. The parameter ΔE fits an equation of the form

$$N_f = A\left(\Delta E\right)^n \tag{1.19}$$

better than $\Delta\Theta_N$ does, although they are related, where N_f is the number of cycles to failure, and A and n are empirically determined constants. [23]

Others, such as P. Kurath[14], have produced work which relates the average, or structural, stress on the specimen. For example, the average shear on the area of the spot-weld may be used. Some success was reported using such methods, but this relies on empirical curve fitting. A life prediction method that is able to predict fatigue behavior and be verified by experimentation seems more readily accepted than one that is based solely on

experimentation. Such methods display an understanding of the failure mechanism(s) at work in the specimens. Empirical relations of the form,

$$F^m N = \text{Constant} \tag{1.20}$$

sometimes prove to be an excellent prediction method for spot-welds, where F is the applied load, N is the number of cycles to failure, and m is a constant having a value nearly equal to three. [35, 43] This equation, as with most empirical relations, has unexplainable limits of validity because the causes of damage are disguised.

1.3.8 Residual stresses

When sheet steel is spot-welded, a small circular portion of the metal is melted. The melted region quickly solidifies as it begins to cool. The cooling of the weld metal, or any metal, causes contraction. This process creates tensile residual stresses about the weld. Studies have found that this tension is distributed radially around the spot-weld and the stress in the sheets goes to zero at the outer and inner faces. [44] The maximum tensile stresses in the sheets, both radially and tangentially, occur very near the inner faces of the steel sheets. [48] Because the greatest tensile stresses occur near the inner faces, the sheets tend to bend toward each other. This secondary effect causes the original crack (or notch) to be pinched together. This compression, whatever its magnitude, would slow or arrest a crack from propagating into the base metal. Perhaps this might mimic a small notch. At higher lives this compressive stress would be harder to overcome and a crack would take longer to grow out of this region, or initiate to a detectable size. This may explain the first stage of life as observed by Lawrence et al. [29]

Once a crack orients itself such that K_I is maximized, the tensile radial and tangential components of residual stress would decrease the life of the specimen. Relieving the residual stress by heat treating offers longer lives. [11] Coining is a method in which the

weld area is crushed together using a punch. [5] This induces compressive residual stresses about the weld, which also yields a longer life. Brinell hardness indentions have also been used to introduce compressive residual stresses in a similar manner.

1.4 Scope of Work

The contributions of F. V. Lawrence, etc., that suggest using a strain-based (notch) approach to study spot-weld fatigue, are ignored here. Instead a crack growth approach will be adopted to solve the problem. Geometry specific work (e.g. only lap joint geometries) has been done to develop crack growth life prediction models. Here a unique model will be developed that can handle any geometry, as long as the loads and moments acting on the spot-weld (of interest) are known. Additional information about the specimen geometry and material properties are also needed. Because of complex geometries and metallurgy, many assumptions will be made to arrive at a life prediction model that is largely closed form.

2. LIFE PREDICTION MODELING

Predicting the fatigue lives of spot-welds can be quite difficult. Assumptions are necessary because the geometry and metallurgical states of a spot-weld can be overwhelming if examined exactly. Assumptions used in this work are generally made to reduce the computations required to predict fatigue lives. A more general model may be developed by relaxing assumptions used (in this paper). The assumptions made, to simplify calculations, for both models developed in this chapter are:

- The weld nugget is cylindrical with a constant radius, "r".
- Residual stresses, although present, are assumed to be small and neglected.
- Failure of a weld means that a crack has grown from the inner surface at the edge of the weld to the outer surface of at least one sheet.
- The crack tends to grow in a small region of the heat affected zone (HAZ) such that the material properties may be considered to be constant.
- The stress intensity factor does not change significantly as the crack grows. Furthermore, the stress intensity of a crack growing out of the original plane of the weld is a function of the original stress intensities
- The angle the crack takes into the sheet metal is constant.
- A threshold value exists for the stress intensity factor such that a crack subjected to a stress intensity less than the threshold will not propagate.

2.1 Constant growth / Maximum opening mode ($K_{II} = 0$)

Previous work has indicated that crack growth remains constant if the sheets of metal are sufficiently thin. According to the Paris power law, this indicates that the stress intensity factors remain constant as the primary crack grows longer. The Paris power law (and the more general Walker equation) is of the form,

$$\frac{da}{dN} = \text{Constant} \tag{2.1}$$

Rearranging and integration of this equation is then a simple matter.

$$\int_{a_i}^{a_f} da = \text{Constant} \int_{N_i}^{N_f} dN \tag{2.2}$$

Equation 2.2 then becomes,

$$a_f - a_i = \text{Constant}(N_f - N_i) \tag{2.3}$$

where for the Walker equation,

$$\text{Constant} = C\left[\frac{\Delta K}{(1-R)^{(1-\gamma)}}\right]^m \tag{2.4}$$

It is assumed that the crack has no initiation stage ($N_i = 0$), so the crack grows from the first cycle, and that there is no re-orientation life ($a_i = 0$), such that the direction of crack growth is in the direction perpendicular to the maximum tensile normal stress. The angle of crack growth, Θ_o, satisfies Eq. 2.5 for K_{III}=0. Most of the failures occur where $K_{III} = 0$ anyway.

$$K_I \sin\Theta_o = -K_{II}(3\cos\Theta_o - 1 \tag{2.5}$$

This equation insures that the in-plane shear stress is zero in the direction of crack propagation. A crack growing under this condition will be growing perpendicular to a principal normal stress, and will have a stable direction if it is the **maximum** tensile normal stress. The angle of the propagating crack will be needed to calculate the final crack length, a_f. The final crack length is given below, using the assumption that the direction of crack propagation remains constant. See Figure 2.1 for a diagram illustrating the relation of a_f, t, and Θ_o.

$$a_f = \frac{t}{\sin\Theta_o} \tag{2.6}$$

Thus, combining Eqs. 2.3, 2.4, and 2.6 gives the following equation.

$$N_f = \frac{t}{C \sin\Theta_o}\left[\frac{\Delta K}{(1-R)^{(1-\gamma)}}\right]^{-m} \tag{2.7}$$

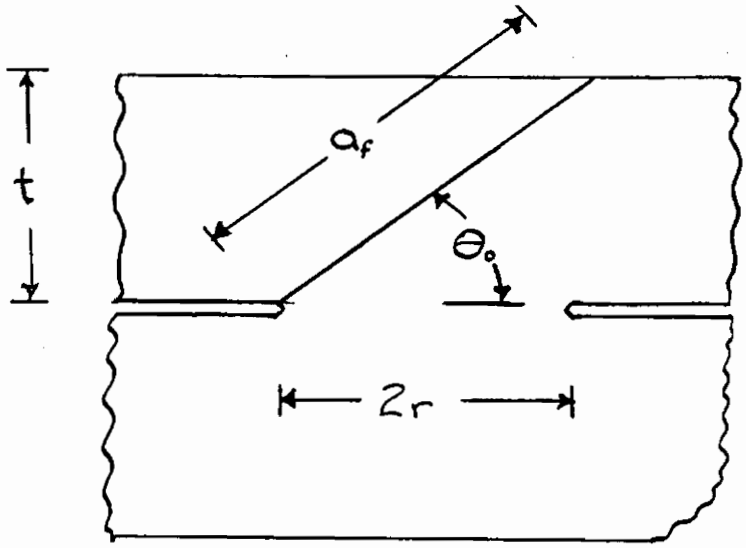

FIGURE 2.1 Diagram showing the relation of a_f, t, and Θ_o.

If the material and geometric constants are known, all that is needed is to calculate ΔK to predict the life of a particular weld. To calculate ΔK, the original stress intensity factors, K_I and K_{II} are used. (Recall that $K_{III} = 0$ is an assumption made for the failure location.) The elastic stress solution for a mixed mode crack is given below.

$$\sigma_{rr} = \frac{K_I}{4\sqrt{2\pi\, r}}\left[5\cos\frac{\Theta}{2} - \cos\frac{3\Theta}{2}\right] + \frac{K_{II}}{4\sqrt{2\pi\, r}}\left[-5\sin\frac{\Theta}{2} + 3\sin\frac{3\Theta}{2}\right] \tag{2.8 a}$$

$$\sigma_{\Theta\Theta} = \frac{K_I}{4\sqrt{2\pi\, r}}\left[3\cos\frac{\Theta}{2} + \cos\frac{3\Theta}{2}\right] + \frac{K_{II}}{4\sqrt{2\pi\, r}}\left[-3\sin\frac{\Theta}{2} - 3\sin\frac{3\Theta}{2}\right] \tag{2.8 b}$$

$$\tau_{r\Theta} = \frac{K_I}{4\sqrt{2\pi\, r}}\left[\sin\frac{\Theta}{2} + \sin\frac{3\Theta}{2}\right] + \frac{K_{II}}{4\sqrt{2\pi\, r}}\left[\cos\frac{\Theta}{2} + 3\cos\frac{3\Theta}{2}\right] \tag{2.8 c}$$

The original stress intensity factors give the stress distribution near the tip of a planar crack. Although the actual crack is three dimensional, it is modeled as two dimensional. This approximation seems reasonable if all crack dimensions are much smaller than the weld diameter. The singular principal normal stress perpendicular to direction of the growing crack, $\sigma_{\Theta\Theta}(\Theta_o)$, is used to calculate the mode I stress intensity factor that drives the crack. There is an assumption that the original stress field is not significantly altered by the presence of a small non-planar crack. This is a necessary assumption for the crack to propagate at a constant rate. For a case where $K_{III}=0$, the following formulation of the stress intensity factor, K , applies. This formulation is valid for an infintesimal kinked crack growing out of the origin of the original two dimensional crack. It is assumed that the kinked crack will be small enough for this expression to be approximately valid.

$$K = \frac{K_I}{4}\left[3\cos\frac{\Theta_o}{2} + \cos\frac{3\Theta_o}{2}\right] - \frac{K_{II}}{4}\left[3\sin\frac{\Theta_o}{2} + 3\sin\frac{3\Theta_o}{2}\right] \qquad (2.9)$$

Since $\pi/2 \le \Theta_o \le 0$, K is positive definite for positive original stress intensity factors. Eq. 2.7 needs the range in the effective mode I stress intensity factor. To obtain this, insert the range in the original stress intensity factors, where the stress intensity factors are in Eq. 2.9. The life of a weld can then be determined from,

$$N_f = \frac{t}{C\sin\Theta_o}\left[\frac{\Delta K_I\left[3\cos\frac{\Theta_o}{2} + \cos\frac{3\Theta_o}{2}\right] - \Delta K_{II}\left[3\sin\frac{\Theta_o}{2} + 3\sin\frac{3\Theta_o}{2}\right]}{4(1-R)^{(1-\gamma)}}\right]^{-m} \qquad (2.10)$$

Recall, that the angle of crack growth, Θ_o, is calculated by Eq. 2.5. Also the stress intensities are calculated using Eqs. 1.15.a and 1.15.b. They have been developed and

have previously been given in Eqs. 1.15 a-c. See Appendix B for a FORTRAN code that has been written to estimate the life of a spot-weld given certain information.

The geometric and material constants applicable to this problem are listed in Table B.2. The material constants used are typical values for the types of steel used. The predicted lives are sensitive to the choice of these constants, so other choices will yield different results. The loads and moments on the spot-weld for each specimen geometry are given in Table B.1. The loads and moments used for this paper assume that the deformation of the specimens are negligible. For box joints, Ford Motor Company has provided the loads and bending moments as seen by the spot-welds. Those loads and moments, listed in Table B.2, are those experienced by the top weld or welds that experience the highest stress intensity. In every test where a weld failure occurred, these top welds failed without exception.

2.2 Constant growth / Minimal life theory $\left(\frac{dN}{d\Theta}=0\right)$

Since life can be written as a function of the angle of crack growth through the sheet metal, Θ, the derivative of this life with respect to Θ will be zero at a minimal value. Starting with Eq. 2.10 and grouping together terms that are not functions of Θ, we obtain the following equation:

$$N_f(\Theta)=\frac{H}{\sin\Theta}\left[L\left(3\cos\frac{\Theta}{2}+\cos\frac{3\Theta}{2}\right)-Q\left(3\sin\frac{\Theta}{2}+3\sin\frac{3\Theta}{2}\right)\right]^{-m} \tag{2.12}$$

where, $H=\frac{t}{C}$, $L=\frac{\Delta K_I}{4(1-R)^{(1-\gamma)}}$, $Q=\frac{\Delta K_{II}}{4(1-R)^{(1-\gamma)}}$.

Taking the first derivative of $N_f(\Theta)$ and setting this to zero gives Eq. 2.13. This formula is valid only for $m\neq -1$.

$$\tan\Theta\left[\frac{L\left(\sin\frac{\Theta}{2}+\sin\frac{3\Theta}{2}\right)+Q\left(\cos\frac{\Theta}{2}+3\cos\frac{3\Theta}{2}\right)}{L\left(3\cos\frac{\Theta}{2}+\cos\frac{3\Theta}{2}\right)-3Q\left(\sin\frac{\Theta}{2}+\sin\frac{3\Theta}{2}\right)}\right]=\frac{2}{3m} \tag{2.13}$$

Finding θ such that Eq. 2.13 is satisfied will give an extreme value, hopefully a minimum value. A closed form solution for Θ looks unlikely so other means will have to be employed. The only difference in this method and the method of the previous section is the way θ is calculated. After this step, the procedure is identical. Similar to what was done for Section 2.1, a FORTRAN code has been written to calculate the life of a spot-weld. The loads and moments, material constants, and geometric constants used are the same as in Section 2.1. See Appendix B for Tables of these data.

This method of minimizing life was developed because life prediction of peel joints using the other method was giving poor results. L. P. Pook derived K_I as a function of shear

and normal forces as well as bending moments. There seems to be no note in the literature indicating that K_{II} is a function of a normal force. For peel joints, where there only exists a normal force, the principle normal stress guides the crack straight through the weld nugget. This is not observed, so an alternate life prediction model had to be created. Cracks in peel joints grow through the sheet metal similar to behavior seen from peel joints. If K_{II} was found to be a function of normal forces and bending moments, the method of the previous section would probably work better. Such analysis requires numerical analysis, which is out of the scope of this work.

3. COMPARISON WITH EXPERIMENTAL DATA

A series of (experimental) tests were performed to verify the life prediction models developed in Chapter 2. Four different specimen types were used; lap, peel, modified peel, and box joints. The most obvious way to collect data from spot-welds as fatigue damage develops, is to simply watch the test while it runs. Typically, a specimen becomes obviously damaged well before failure, and several stages of damage can be defined. A major limitation of this method is that cracks tend to initiate on the inner surface where they evade visual detection. For the fatigue tests performed, the following stages of damage were reported where possible:

- First visible surface crack, usually 0.5 mm to 1 mm surface length.
- 1/4 circumference crack, when the surface crack has progressed until it arcs around one fourth of the weld circle. If the crack does not circle the weld, then this stage of damage is reported when the crack grows into the base metal.
- Failure (rupture), where the specimen is pulled into two pieces. If the testing machine deflection limits stop the test on the verge of rupture, then that life is used.

3.1. Peel Joints

Peel joint and modified peel joint testing was performed by gripping the ends of the specimen 0.75 inches deep in the wedge grips of an MTS machine. See Figure 3.1 for a photo of a peel joint specimen loaded in the grips and ready for testing. Some of the peel joint specimens were modified by bending the welded tabs from the original 90 degrees to 45 degrees from the path of loading. This modification was made to further test the life prediction methods developed in the previous chapter. See Figure 3.2 for sketches of both original and modified peel joint geometries.

The minimal life method, $\frac{dN}{d\Theta} = 0$, was developed because the maximum K_I method was giving poor results for peel joints. The angle of crack growth, Θ_o, found by maximizing K_I, was zero, which had the crack growing into the weld. Since the crack grows through the sheet metal, that result was deemed unacceptable. No information was found in the literature where a normal force, F_3, would cause a mode II stress intensity, K_{II}. If this was true then the crack would grow out of the plane of the weld. Peel joints were predicted using the minimal life method of Section 2.2. There seems to be no reason why a crack would grow in the direction such that the life would be shortest, as long as linear elastic fracture mechanics applies.

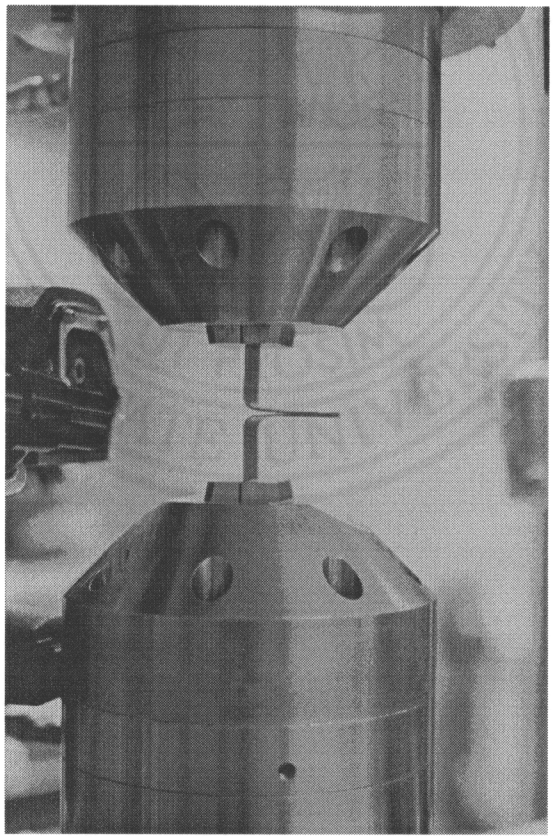

FIGURE 3.1. Photo of peel joint specimen in grips of MTS machine.

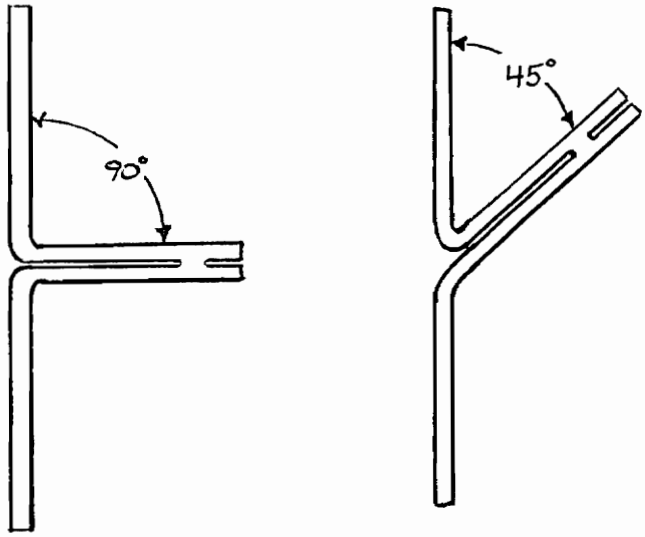

FIGURE 3.2 Sketches of original and modified peel joint geometries.

3.1.1. Data Tables

The results of the fatigue tests of the peel specimens are shown in Table 3.1 and 3.2 for 1010 steel and 950X steel, respectively. The specimens were assigned specimen numbers to help keep track of data (e.g. P1-107). The first letter stands for the type of specimen (P=peel joint, L=lap joint, T=box joint). The number after the letter indicates the type of material (1=1010 steel, 9=950X steel). Finally, after the dash is a three digit number such that each specimen has a unique specimen number. The three digit number after the dash indicates which of three batches the specimen is a member of. Specimen numbers starting with 100 are from the second batch of specimens sent from Ford Motor Company. Those starting with 200 are from the third batch of specimens. The first batch was found to be of poor quality so the results of those tests are not used. Blank spaces in the data tables indicate the data are unavailable or not applicable.

TABLE 3.1 - DATA FOR 1010 STEEL PEEL JOINTS

Specimen	Max. load (lbf.)	Load ratio	Rate (Hz.)	First crack (cycles)	1/4 circ. (cycles)	Failure (cycles)
P1-101	563				1(Static load)	
P1-102	150	0.1	4	13,000	14,350	17,115
P1-103	150	0.1	4			13,658
P1-104	175	0.1	4	9,750	14,000	16,286
P1-105	210	0.1	4	4,900	5,300	5,988
P1-106	250	0.1	2	2,050	3,150	4,187
P1-107	100	0.1	4	7,400	8,600	17,734
P1-108	50	0.1	4			71,069
P1-109	45	0.1	4	105,000	107,500	124,324
P1-110	45	0.1	4	90,000	99,000	115,060
P1-111	100	0.1	1			12,002
P1-112	50	0.1	2			31,276
P1-113	40	0.1	2.5			317,889
P1-114	35	0.1	3	250,000		315,081
P1-115	30	0.1	3	455,000	585,000	605,667
P1-116	25	0.1	3	440,000		557,552
P1-117	20	0.1	5			>3,000,000
P1-118	60	0.5	2.5			198,218
P1-119	40	0.5	5	850,000	900,000	977,108
P1-120	50	0.5	3	400,000		502,000
P1-121	70	0.5	2	78,000		97,313
P1-122	110	0.5	1.5			50,479
P1-123	120	0.75	3	475,000		1,274,149
P1-124	140	0.75	1		450,000	549,006
P1-125	160	0.75	5	420,000	500,000	627,527
P1-126	200	0.75	1	250,000	320,000	363,946
P1-127	240	0.75	3	205,000		219,151
P1-128	280	0.75	2.5			89,062
P1-129	300	0.75	2.5	100,000		176,030
P1-201	160	0.5	2.5	31,000	42,000	47,279
P1-202	240	0.75	2			142,792
P1-203	200	0.75	3	100,000	120,000	180,741
P1-204	300	0.75	1	10	50	94
P1-205	270	0.75	1			90,422
P1-206	55	0.5	4	270,000	350,000	461,476
P1-207	23	0.1	5	760,000	950,000	1,110,930
P1-208	290	0.75	1			3206
P1-209	160	0.5	3			77,613
P1-210	200	0.5	2			30,957
P1-211	300	0.1	1	1100	1175	1221
P1-212	320	0.1	1	375	430	473
P1-213	300	0.5	2	900	950	964
P1-214	290	0.5	2	2300	2450	2566
P1-215	130	0.75	3	300,000	390,000	662,111
P1-216	45	0.5	3	450,000	500,000	623,249
P1-217	250	0.5	0.5	5200		5477
P1-218	295	0.5	0.25	2000	2500	4413
P1-219	38	0.5	5			582,096
P1-220	292	0.75	0.5	80	500	1818
MODIFIED PEEL JOINTS (45 degree angle)						
P1-221	80	0.1	1			13,342
P1-222	60	0.1	1			27,217
P1-223	50	0.1	1.5			47,393
P1-224	40	0.1	2			68,027
P1-225	30	0.1	2	540,000		585,072
P1-226	27	0.1	5	3,000,000		3,409,833
P1-227	90	0.1	1	6,000	7,200	11,673
P1-228	28	0.1	3	1,500,000	1,580,000	1,630,514
P1-229	100	0.1	0.5	8,500	11,200	11,958
P1-230	120	0.1	0.5	8,000	10,000	11,343

TABLE 3.2 - DATA FOR 950X STEEL PEEL JOINTS

Specimen	Max. load (lbf.)	Load ratio	Rate (Hz.)	First crack (cycles)	1/4 circ. (cycles)	Failure (cycles)
P9-101	430				1 (Static load)	
P9-102	150	0.1	4	800	1,000	3,209
P9-103	150	0.1	4	900	1,700	4,018
P9-104	120	0.1	4	1,300	3,800	6,789
P9-105	120	0.1	4	1,250	3,000	5,187
P9-106	90	0.1	4	4,200	5,100	10,093
P9-107	70	0.1	4	16,000	19,000	25,426
P9-108	50	0.1	4			90,345
P9-109	50	0.1	4			85,216
P9-110	50	0.1	4	72,100	78,633	91,492
P9-111	40	0.1	2.5	120,000	130,000	143,917
P9-112	50	0.1	2			24,199
P9-113	40	0.1	2	75,000	77,000	79,394
P9-114	35	0.1	4	130,000	140,000	146,493
P9-115	30	0.1	5	255,000	275,000	285,513
P9-118	25	0.1	5	580,000	650,000	681,511
P9-119	20	0.1	5	1,000,000	1,250,000	1,352,806
P9-120	60	0.5	5	150,000	180,000	210,734
P9-121	40	0.5	5			1,241,945
P9-122	80	0.5	1.75	50,000		78,718
P9-123	100	0.5	0.6	10,000		23,258
P9-124	50	0.5	5	255,000		371,710
P9-125	70	0.5	2	180,000	216,000	221,300
P9-126	90	0.5	3	50,000		62,626
P9-127	100	0.75	3	250,000	310,000	426,873
P9-128	150	0.5	3	5,600	11,000	14,060
P9-129	160	0.5	2	5,300	9,600	12,298
P9-201	140	0.75	3	120,000	170,000	208,213
P9-202	50	0.5	5			615,000
P9-203	30	0.1	4		205,000	228,748
P9-204	45	0.1	4	18,000	23,000	24,996
P9-205	27	0.1	7	480,000	600,000	635,490
P9-206	45	0.5	5	475,000	560,000	592,407
P9-207	80	0.75	5		1,100,000	1,966,276
P9-208	120	0.75	4	220,000	340,000	390,764
P9-209	140	0.75	4	165,000	200,000	237,657
P9-210	160	0.75	4	120,000		194,443
P9-211	200	0.75	5	55,000	65,000	76,882
P9-212	240	0.75	4			114,608
P9-213	300	0.75	1			553
P9-214	200	0.5	1			17,614
P9-215	90	0.75	3	435,000	550,000	1,116,517
P9-216	200	0.1	0.5	900	1100	1252
P9-217	250	0.5	0.5	1900	2550	2971
P9-218	270	0.75	4	39,000	50,000	63,673
P9-219	300	0.5	0.5	1800		3,676
P9-220	280	0.5	0.5	5	140	157
P9-221	44	0.5	3	600,000	750,000	876,825
P9-222	280	0.75	0.5	40,000		72,414
P9-223	290	0.75	0.5	28,000	29,500	30,182
MODIFIED PEEL JOINTS (45 degree angle)						
P9-224	50	0.1	2	90,000		123,129
P9-225	30	0.1	2.5	705,000		803,556
P9-226	40	0.1	3	325,000		363,884
P9-227	60	0.1	2	50,000	62,000	75,944
P9-228	70	0.1	2	20,000		25,535
P9-229	80	0.1	1	18,000		25,678
P9-230	100	0.1	1	6,000		9,338
P9-231	28	0.1	5	575,000	620,000	660,713
P9-232	35	0.1	5	290,000	350,000	383,558
P9-233	120	0.1	1	1,500	3,000	3,745

3.1.2. Load-Life Data

When the data of Table 3.1 and 3.2 are plotted on a log-log plot, a trend in the data similar to S-N curves is noted. As stress (or in this case load) is increased, the life decreases. Load is used instead of stress for the vertical coordinate of these plots because there is no obvious area to use for calculating a stress. An equation of the form below can be fitted to the data using a least squares method.

$$N = AF^B \qquad \text{(Fitted line)} \qquad (3.1)$$

The predicted (or theoretical) line is given by Eq. 3.2. All four constants, A, B, C, and D can be found in the upper right corner of each load-life plot. The units of these constants are not given, but have been developed using force, F, in lbf. and life, N, in cycles.

$$N = CF^D \qquad \text{(Theoretical line)} \qquad (3.2)$$

F is the maximum applied load (for constant amplitude cycling), N is the number of cycles to failure. Since some of the data points for first cracking and 1/4 circumference cracking are missing, only rupture failures (pulled in two or more pieces) are used. A description of each plot is given below.

TABLE 3.3 DESCRIPTION OF LOAD-LIFE PLOTS FOR PEEL JOINTS

FIGURE NUMBER	MATERIAL	LOAD RATIO, R	GEOMETRY
FIGURE 3.3	SAE 1010 steel	0.1	Original
FIGURE 3.4	SAE 950X steel	0.1	Original
FIGURE 3.5	SAE 1010 steel	0.5	Original
FIGURE 3.6	SAE 950X steel	0.5	Original
FIGURE 3.7	SAE 1010 steel	0.75	Original
FIGURE 3.8	SAE 950X steel	0.75	Original
FIGURE 3.9	SAE 1010 steel	0.1	Modified
FIGURE 3.10	SAE 950X steel	0.1	Modified

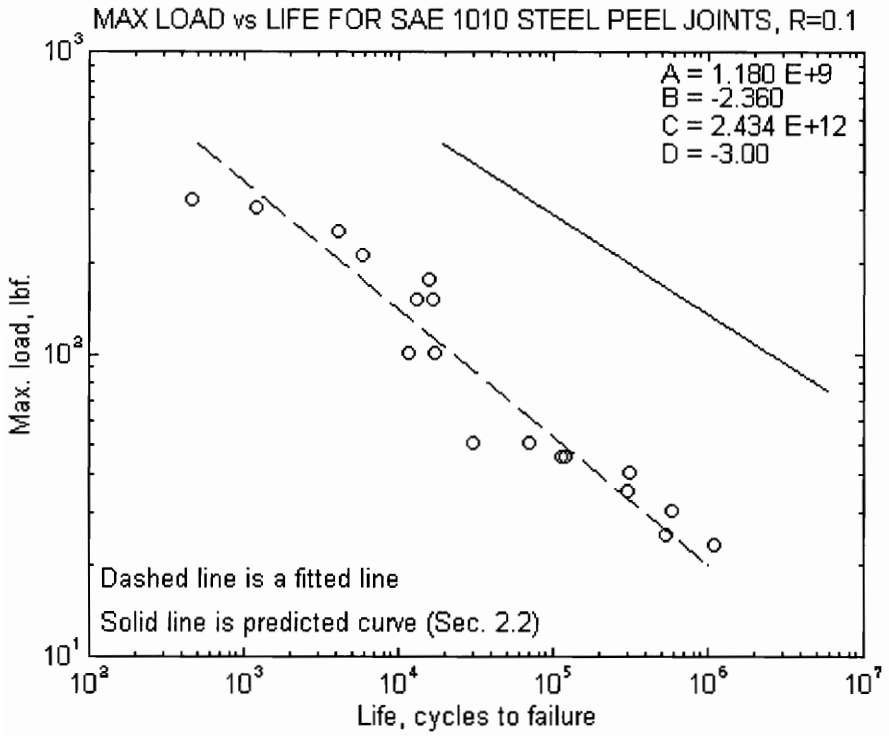

Figure 3.3 Load-life data for SAE 1010 steel peel joints, R=0.1.

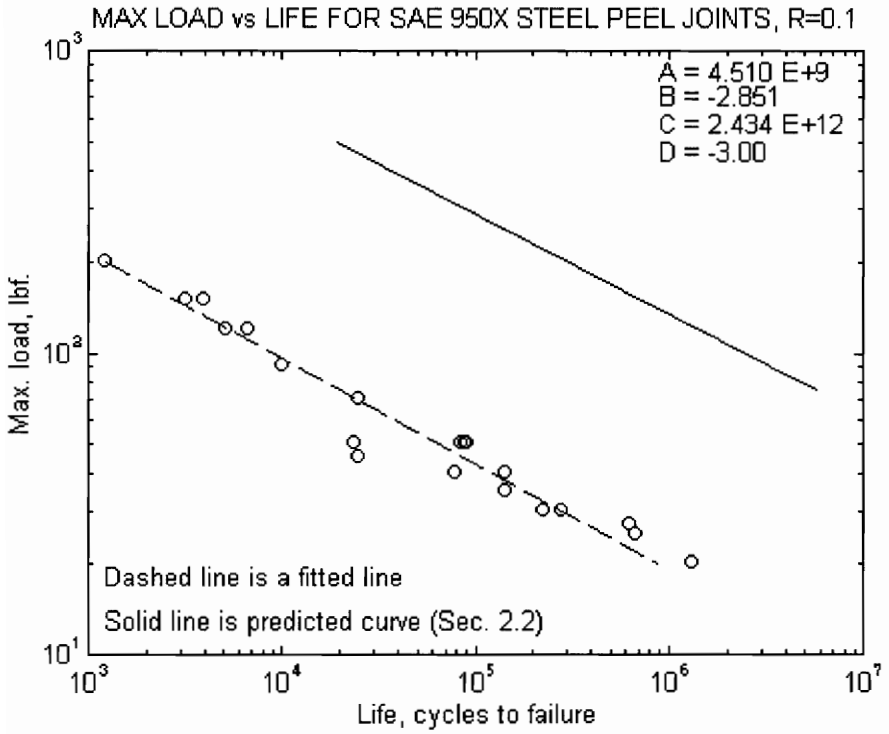

Figure 3.4 Load-life data for SAE 950X steel peel joints, R=0.1

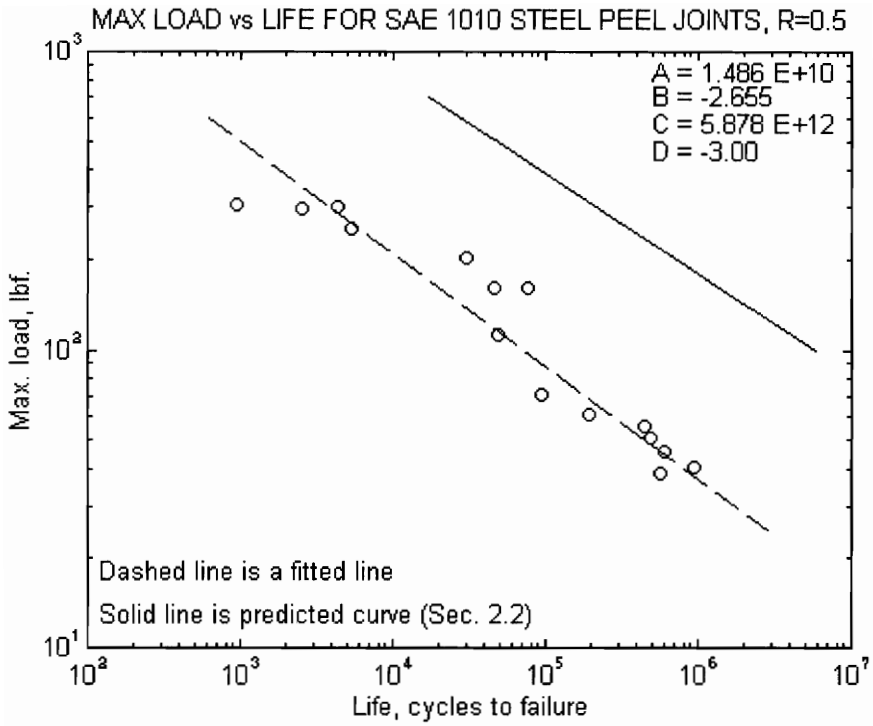

Figure 3.5 Load-life data for SAE 1010 steel peel joints, R=0.5

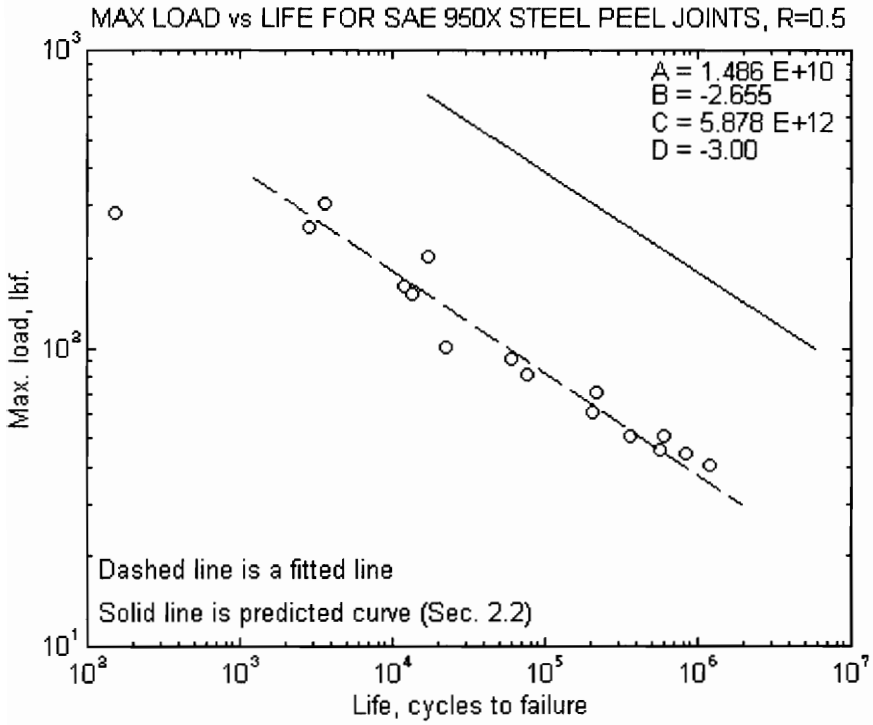

Figure 3.6 Load-life data for SAE 950X steel peel joints, R=0.5

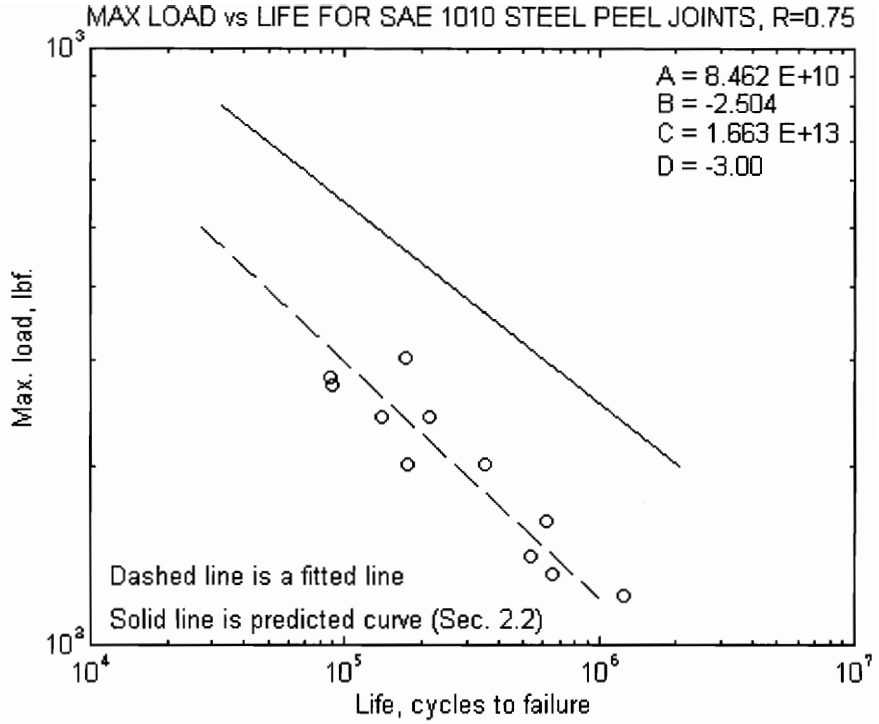

Figure 3.7 Load-life data for SAE 1010 steel peel joints, R=0.75

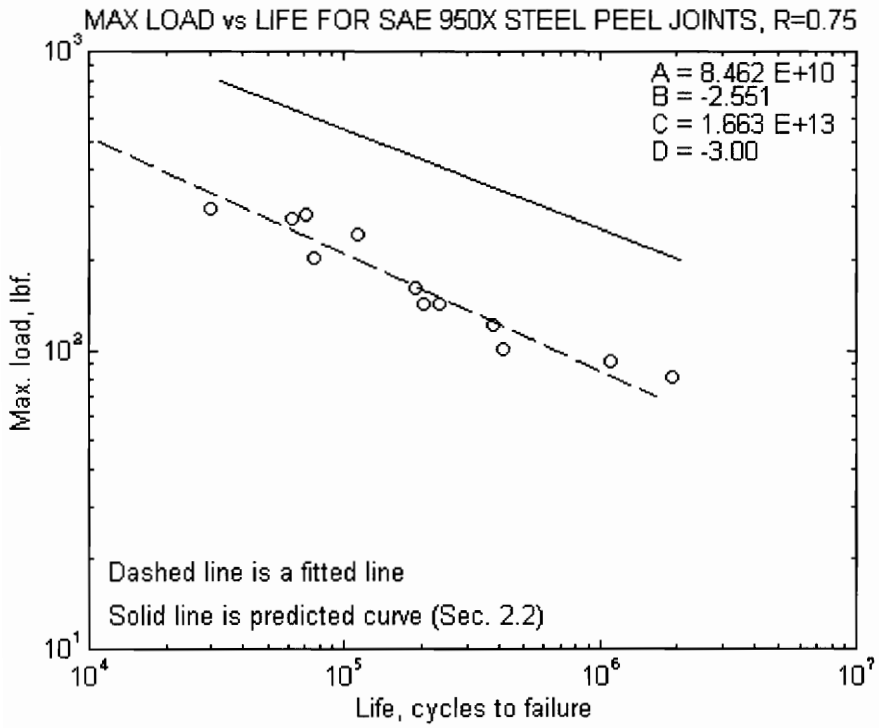

Figure 3.8 Load-life data for SAE 950X steel peel joints, R=0.75

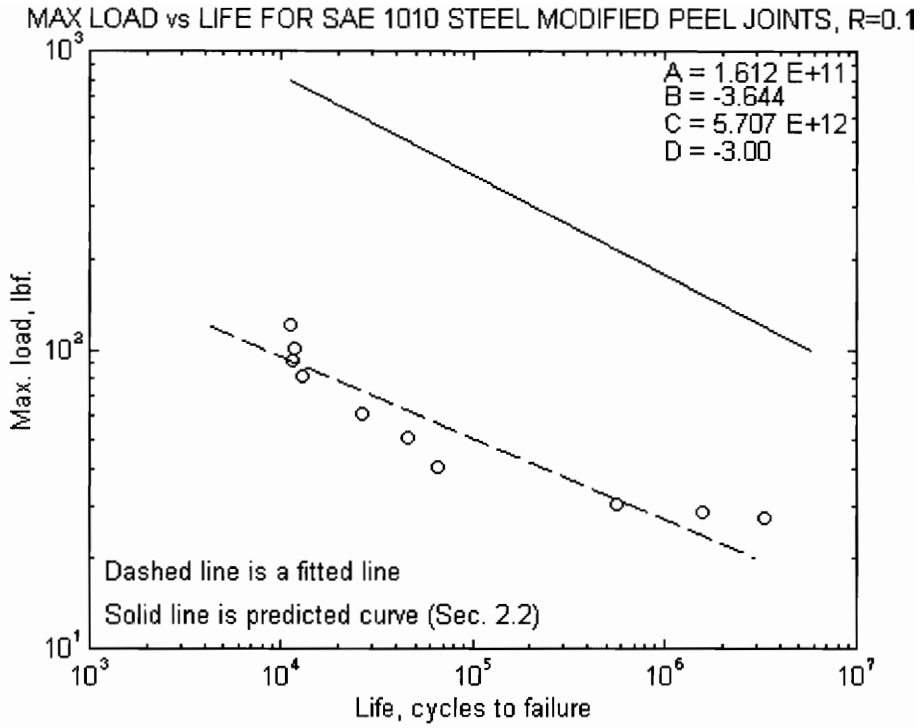

Figure 3.9 Load-life data for SAE 1010 steel modified peel joints, R=0.1

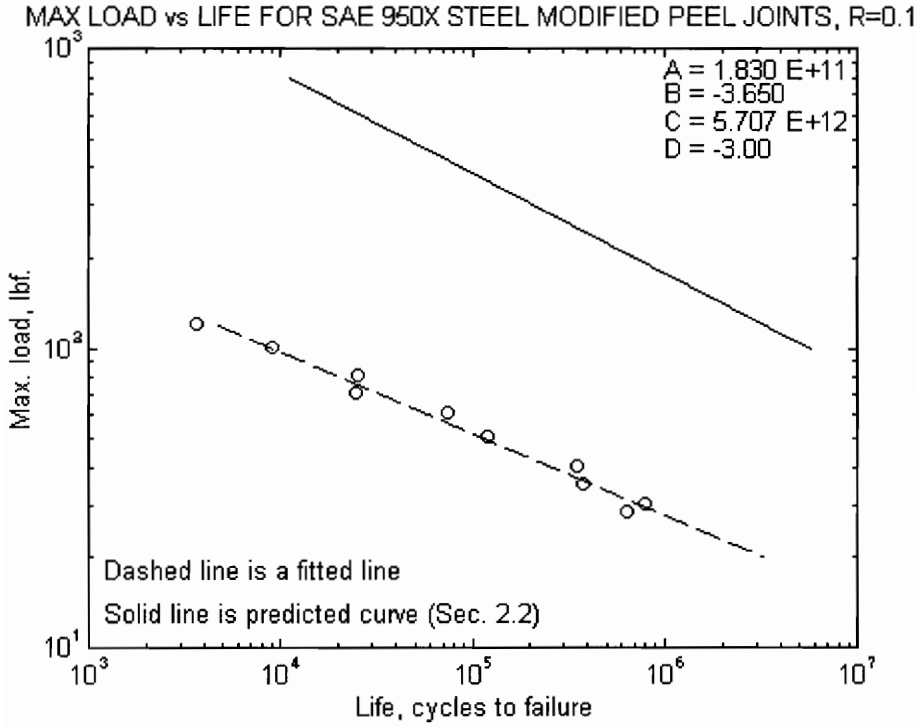

Figure 3.10 Load-life data for SAE 950X steel modified peel joints, R=0.1

3.2. Lap Joints

In a similar fashion to the peel joints, the ends of the lap joints were also gripped 0.75 inches deep in the wedge grips of an MTS machine. However, due to the anti-symmetric geometry of the specimens, a small spacer was glued to one side of each end unless a spacer was already welded in place. This eliminated a small bending moment in the specimens due to the opposite sides of that specimen not being coplanar. See Figure 3.11 for a side view of a lap joint specimen. The testing of lap joints was similar to that of peel joints.

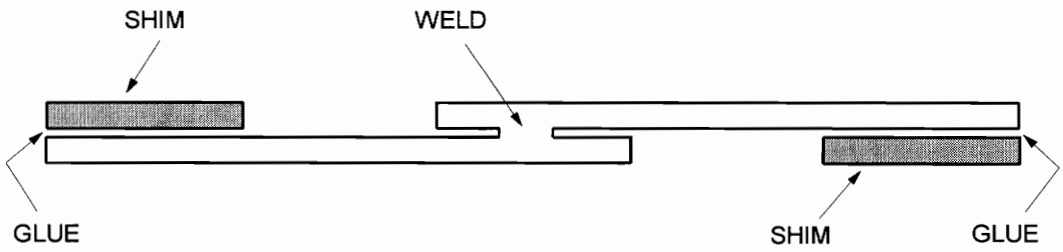

FIGURE 3.11 Sketch of lap joint specimen after shims were added.

3.2.1. Data Tables

The results of the fatigue tests described above are displayed in Tables 3.4 and 3.5, for 1010 steel and 950X steel respectively. Blank spaces means the data are unavailable or not applicable. At this time some of the lap joints have yet to be tested. These specimens are to be tested by another student at a later date.

TABLE 3.4 - DATA FOR 1010 STEEL LAP JOINTS

Specimen	Max. load (lbf.)	Load ratio	Rate (Hz.)	First crack (cycles)	1/4 circ. (cycles)	Failure (cycles)
L1-101	1823				1 (Static load)	
L1-103	900	0.1	10	6,000	11,500	25,499
L1-104	900	0.1	10	12,000	18,000	30,511
L1-105	650	0.1	10	23,000	46,000	109,563
L1-106	470	0.1	10	21,000	35,000	534,000
L1-107	470	0.1	10	107,000	210,000	466,753
L1-108	350	0.1	10	794,000	1,424,000	2,285,178
L1-109	1150	0.1	10	8,000	9,500	9,663
L1-110	350	0.1	10	575,000	932,000	1,555,650
L1-203	1700			Static test		1
L1-204	1680			Static test		1
L1-205	600	0.5	10	400,000	475,000	502,987
L1-206	800	0.5	5	220,000		242,420
L1-207	1000	0.5	10			77,972
L1-208	600	0.1	10		100,000	100,042
L1-209	1200	0.5	1	62,000		62,165
L1-210	400	0.5	20			>6,800,000
L1-211	1300	0.5	3			46,300
L1-212	800	0.75	30			>6,800,000
L1-213	1200	0.75	10	640,000	670,000	682,433
L1-216	1300	0.75	10	550,000	580,000	580,237
L1-217	1400	0.75	5	315,000		324,050
L1-218	1200	0.1	5	11,000		11,607
L1-219	1400	0.1	10	5200	5300	5325
L1-220	500	0.5	30			>6,800,000
L1-221	400	0.1	10	450,000	475,000	483,004
L1-222	1250	0.1	10	11,400	11,600	11,686
L1-223	1500	0.1	10	680	688	694
L1-224	550	0.5	30			2,809,075
L1-225	1600	0.75	10	342	342	342

TABLE 3.5 - DATA FOR 950X STEEL LAP JOINTS

Specimen	Max. load (lbf.)	Load ratio	Rate (Hz.)	First crack (cycles)	1/4 circ. (cycles)	Failure (cycles)
L9-101	2654				1 (Static load)	
L9-103	950	0.1	10			18,946
L9-104	950	0.1	10			20,277
L9-105	1300	0.1	10			6,091
L9-106	500	0.1	10			224,157
L9-107	500	0.1	10			296,300
L9-108	370	0.1	10	300,000	365,000	407,968
L9-109	1300	0.1	10	4,000	5,000	6,355
L9-110	700	0.1	10	14,000	45,000	67,653
L9-111	700	0.1	10	11,200	32,000	53,350
L9-112	370	0.1	10	450,000	650,000	759,879
L9-118	1000	0.1	10			7,448
L9-201	2030		Static loading			1
L9-202	2060		Static loading			1
L9-204	1000	0.5	10	58,000	63,000	63,591
L9-205	1200	0.5	10	27,000	31,000	31,863
L9-206	800	0.5	10	165,000	180,000	190,296
L9-207	600	0.5	10	490,000	525,000	555,228
L9-208	400	0.5	20	3,600,000		4,071,942
L9-209	1400	0.5	5	17,000	19,000	19,400
L9-213	1200	0.1	10			4985
L9-215	1200	0.1	10	6,700	6,743	6,743
L9-216	1100	0.1	10			5,543
L9-217	1100	0.1	10	5,700	5,804	5,804
L9-221	1800	0.5	10	2,270	2,270	2,270
L9-222	1800	0.1	10	454	454	454
L9-223	350	0.1	25			968,419
L9-224	1600	0.1	10	1,297	1,297	1,297
L9-225	1600	0.75	20	126,000	131,000	131,749
L9-226	1800	0.75	20	61,000	61,042	61,042
L9-227	1200	0.75	25			380,354

3.2.2. Load-Life Data

Analogous to Section 3.1.2. for peel joints, in this section load-life plots for lap joints are displayed in Figures 3.11 through 3.14. Table 3.6 lists a description of each of the lap joint load-life plots. Constants for Eqs. 3.1 and 3.2 appear in the upper right corner of each load-life plot.

TABLE 3.6 DESCRIPTION OF LOAD-LIFE PLOTS FOR LAP JOINTS

FIGURE NUMBER	MATERIAL	LOAD RATIO, R
FIGURE 3.12	SAE 1010 steel	0.1
FIGURE 3.13	SAE 950X steel	0.1
FIGURE 3.14	SAE 1010 steel	0.5
FIGURE 3.15	SAE 950X steel	0.5

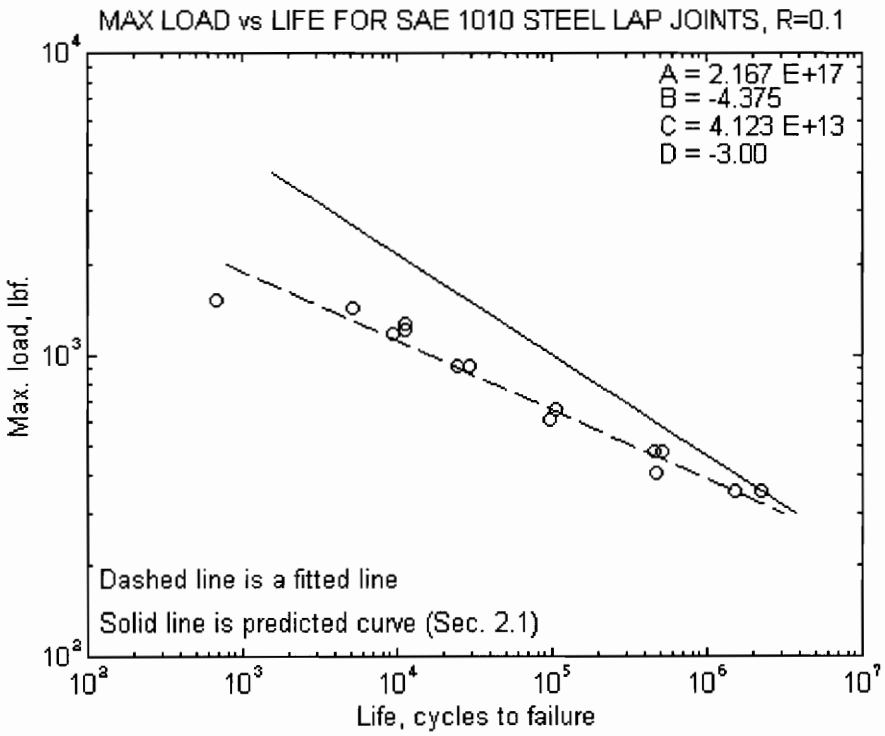

FIGURE 3.12 - S-N type data for SAE 1010 steel lap joints, R=0.1

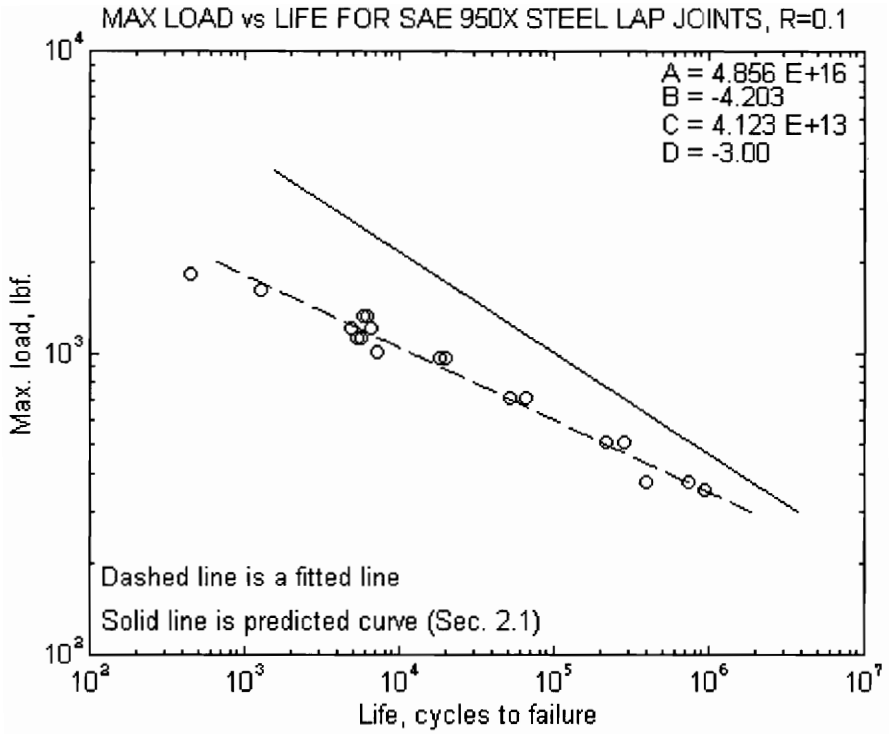

FIGURE 3.13 - S-N type data for SAE 950X steel lap joints, R=0.1

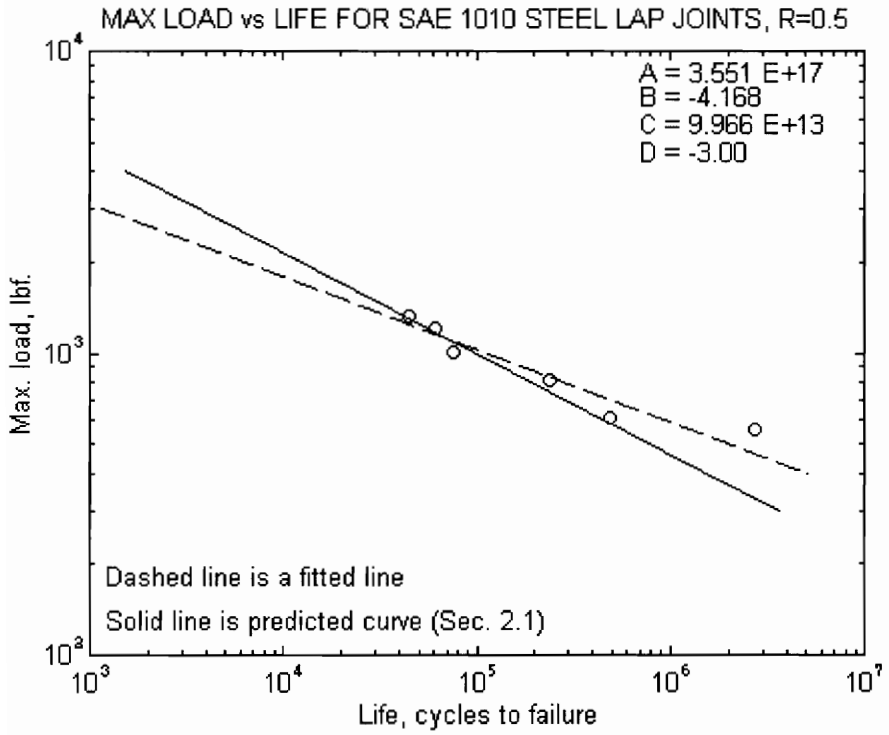

FIGURE 3.14 - S-N type data for SAE 1010 steel lap joints, R=0.5

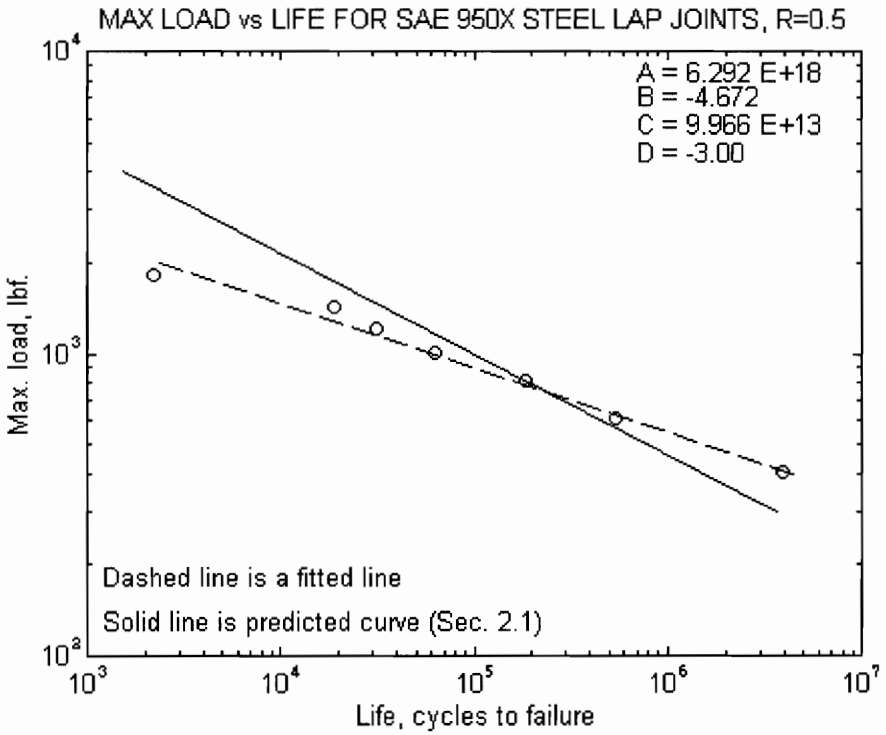

FIGURE 3.15 - S-N type data for SAE 950X steel lap joints, R=0.5

3.3. Box Joints

Box joints are unique from the other specimens because they have multiple welds and are small structures. The box specimen geometry complicated testing. A test fixture needed to be constructed to hold the two back plates fixed while applying a load to the free or forward end. Details of the test fixture are given in Appendix A.

3.3.1. Test Fixture

The sponsor wanted to cyclically load the box joints in two different modes. First was a bending only mode. Although this loading is not strictly bending only, since shear loads are also present, it will be called bending only. For this report, bending only means that there is no torsion applied. A cantilevered rod was fabricated so the testing machine could apply its load six inches from the end of a box joint specimen's free end on the centerline of the specimen. Second was a combined bending and torsion mode. In this case the load was applied six inches in front of the specimen as in the bending only mode, but the point of loading was moved an additional six inches to the side. These point of loading dimensions were suggested by the sponsor. See Figure 3.16 for details of the loading. Appendix A provides details of the testing fixture created for testing box joints. It is hoped that anyone needing to test these specimens in the future will be able to use a similar test fixture.

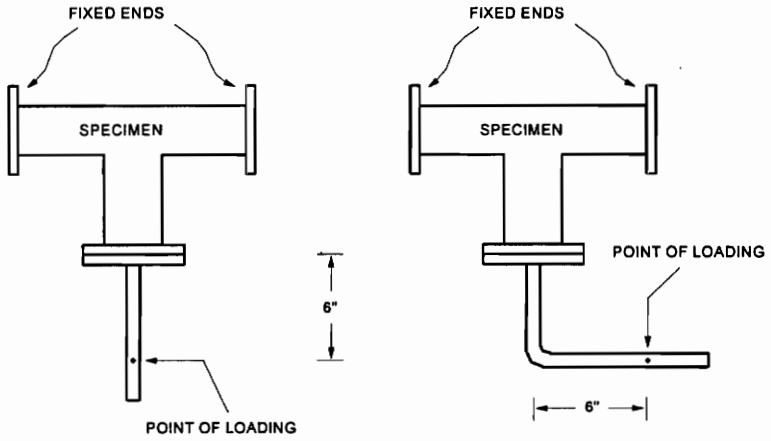

FIGURE 3.16 Sketches of two types of box joint specimen loadings;
(Right) Bending only
(Left) Bending and torsion

A test fixture was needed that could hold a specimen the proper distance from the line the actuator travels. Also, the same fixture needed to handle both loading scenarios. See Figure 3.17 for a photo of the assembled test fixture in place with a box joint specimen ready for testing. Note that this photo is of the bending only test setup. Appendix A contains other photographs and drawings of the box joint test fixture.

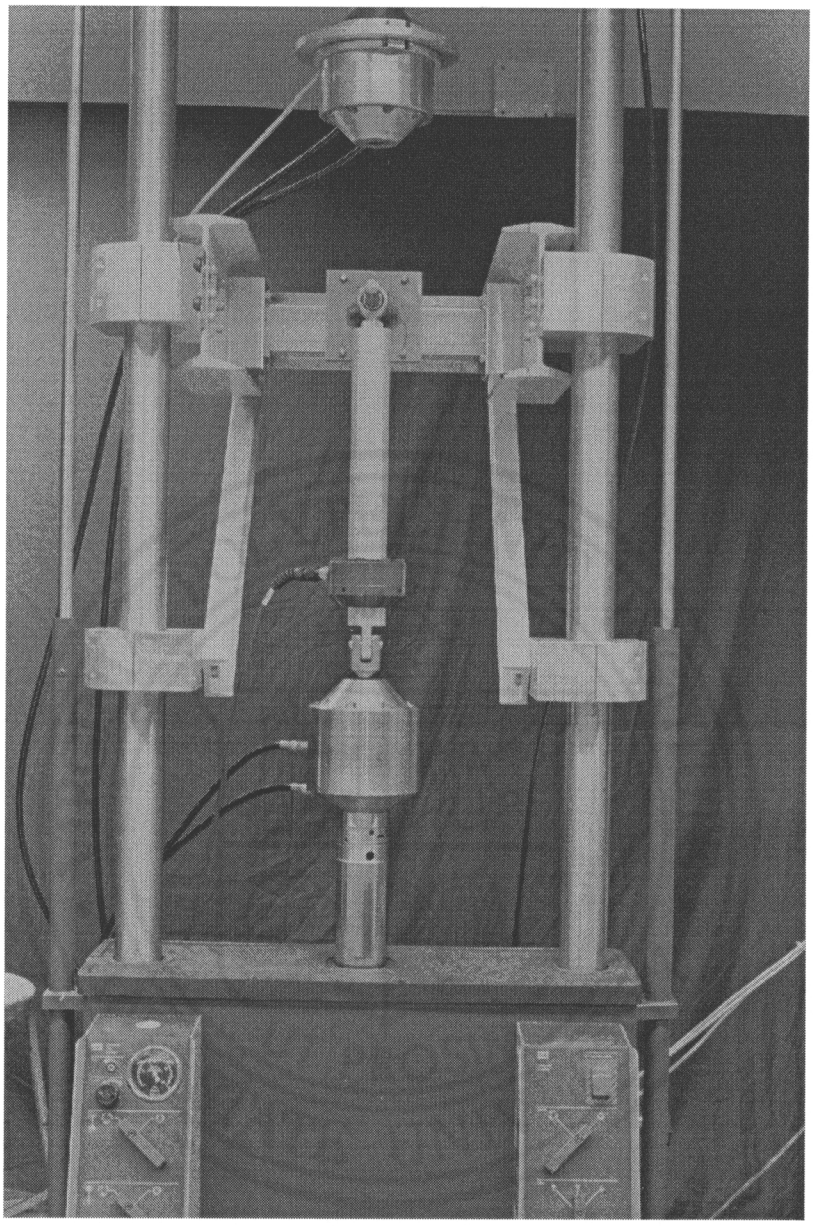

FIGURE 3.17 Photo of assembled test fixture, bending only case, front view.

3.3.2. Data Tables

The data generated from the tests described above are listed in Tables 3.7 and 3.8, for 1010 steel and 950X steel, respectively. All specimens did not fail in the same way. Specimens were considered failed due to excessive deflection of the actuator (1.75

inches), but some failed because of fatigue cracks originating at the spot-welds, while others buckled. See Figures 3.18 and 3.19 for photos of the two failure types. Due to lack of access to both sides of the spot-welds, and the tendency of cracks to initiate on the hidden side, the various damage stages were not observed, with the exception of failure (rupture).

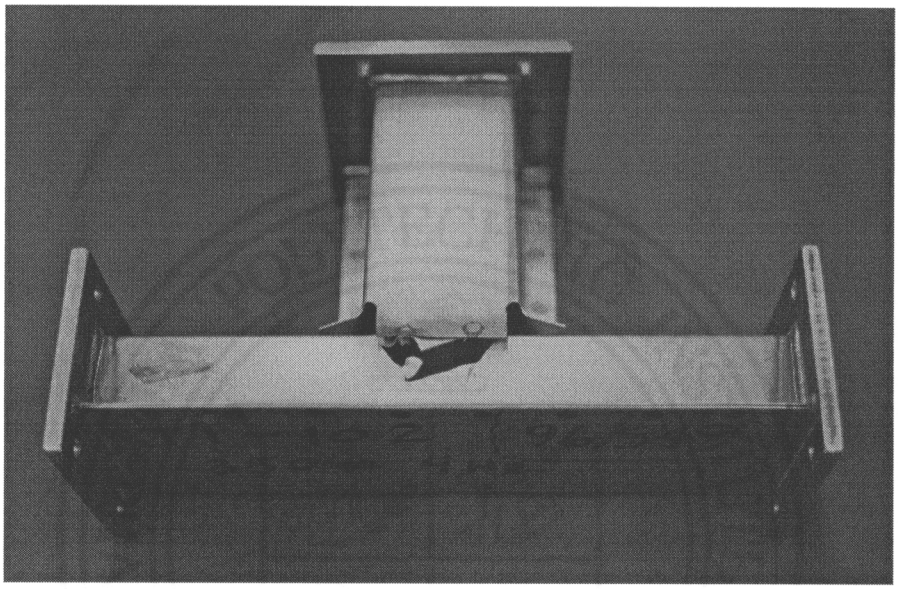

FIGURE 3.18 Box joint specimen that failed due to cracks around welds (top view).

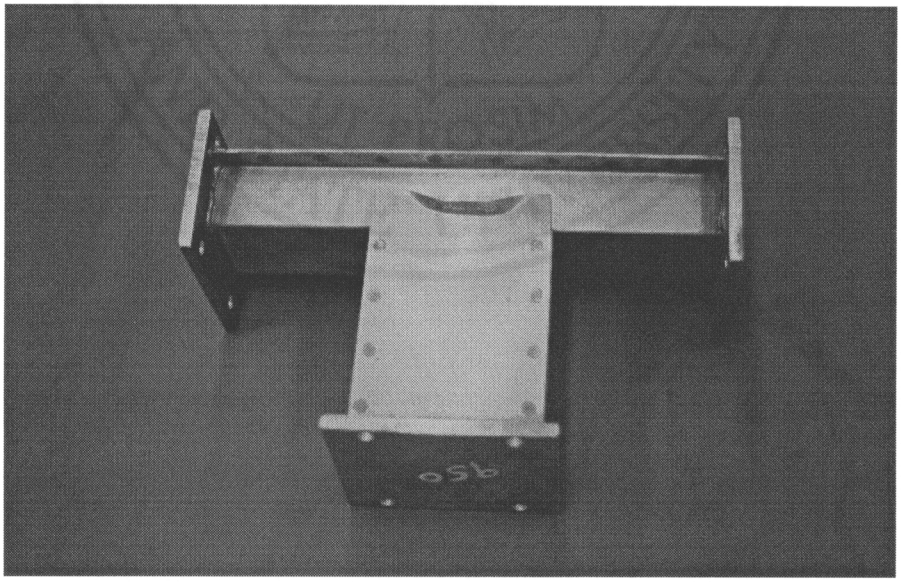

FIGURE 3.19 Box joint specimen that failed due to buckling (bottom view).

TABLE 3.7 - DATA FOR 1010 STEEL BOX JOINTS

Specimen	Max. load (lbf.)	Load ratio R	Rate (Hz.)	Failure (cycles)	Type of Failure
(BENDING ONLY MODE)					
T1-101	475		Static test		Buckling
T1-102	350	0.1	4	96,549	Weld failure
T1-103	200	0.1	4	2,730,000	Stopped
T1-104	350	0.1	4	104,761	Weld failure
T1-105	450	0.1	1	542	Buckling
T1-106	450	0.1	1	171	Buckling
T1-201		Destroyed in testing accident			Buckling
T1-202	400	0.1	1.5	53,388	Weld Failure
T1-203	400	0.1	1	44,492	Weld Failure
T1-204	375	0.1	1.5	66,306	Weld Failure
T1-205	375	0.1	1.5	62,058	Weld Failure
T1-206	350	0.1	2	105,804	Weld Failure
T1-207	325	0.1	2	119,265	Weld Failure
T1-208	325	0.1	3	91,433	Weld Failure
T1-209	275	0.1	4	309,273	Weld Failure
T1-210	250	0.1	5	603,031	Weld Failure
T1-211	250	0.1	6	587,178	Weld Failure
(BENDING AND TORSION MODE)					
T1-107	420		Static test		Buckling
T1-108	350	0.1	1.5	70,434	Buckling
T1-109	350	0.1	2	506	Buckling
T1-212	300	0.1	1	162,362	Weld failure
T1-213	250	0.1	1	300,533	Weld failure
T1-214	400	0.1	0.25	23,718	Weld failure
T1-215	225	0.1	5	581,752	Weld failure
T1-216	420	0.1	5	38,653	Weld failure
T1-217	200	0.1	8	973,669	Weld failure

TABLE 3.8 - DATA FOR 950X STEEL BOX JOINTS

Specimen	Max. load (lbf.)	Load ratio R	Rate (Hz.)	Failure (cycles)	Type of Failure
(BENDING ONLY MODE)					
T9-101	725		Static test		Buckling
T9-102	300	0.1	4	112,547	Weld failure
T9-103	300	0.1	4	116,873	Weld failure
T9-104	450	0.1	2	41,696	Weld failure
T9-105	650	0.1	1	8,637	Weld failure
T9-106	650	0.1	1	4,423	Buckling
T9-201	250	0.1	6	264,037	Weld Failure
T9-202	275	0.1	5	350,716	Weld Failure
T9-203	250	0.1	5	255,963	Weld Failure
T9-204	325	0.1	2.5	123,255	Weld Failure
T9-205	375	0.1	1.5	67,086	Weld Failure
T9-206	425	0.1	1	29,758	Weld Failure
T9-207	475	0.1	0.75	14,388	Weld Failure
T9-208	525	0.1	0.4	9,273	Weld Failure
T9-209	600	0.1	0.3	6,462	Weld Failure
T9-210	400	0.75	10	>3,800,000	Stopped
T9-211	450	0.5	2.5	222,327	Weld Failure
T9-212	550	0.5	1	65,076	Weld Failure
T9-213	600	0.5	1	44,344	Weld Failure
T9-214	400	0.5	5	22,262	Weld Failure
T9-215	300	0.5	10	570,868	Weld Failure
(BENDING AND TORSION MODE)					
T9-107	680		Static test		Buckling
T9-108	450	0.1	2	30,113	Weld failure
T9-109	450	0.1	2	24,519	Weld failure
T9-110	550	0.1	1	10,725	Weld failure
T9-216	325	0.1	1	90,913	Weld failure
T9-217	400	0.1	1	41,025	Weld failure
T9-218	300	0.1	3	82,527	Weld failure
T9-219	250	0.1	5	246,498	Weld failure
T9-220	200	0.1	3	856,212	Weld failure
T9-221	600	0.1	0.5	2,303	Weld failure

3.3.3. Load-Life Data

Similar to peel and lap joints, the data for box joints were displayed on a log-log plot in Figures 3.20 through 3.24. The plots are similar to those of Sections 3.1.3 and 3.2.3. A description of the plots are given in Table 3.9. Again, constants for Eqs. 3.1 and 3.2 are given in the upper right hand corner of each plot.

TABLE 3.9 DESCRIPTION OF LOAD-LIFE PLOTS FOR BOX JOINTS

FIGURE NUMBER	MATERIAL	LOAD RATIO, R	MODE OF LOADING
FIGURE 3.20	SAE 1010 steel	0.1	Bending only
FIGURE 3.21	SAE 950X steel	0.1	Bending only
FIGURE 3.22	SAE 1010 steel	0.5	Bending only
FIGURE 3.23	SAE 1010 steel	0.1	Bending and Torsion
FIGURE 3.24	SAE 950X steel	0.1	Bending and Torsion

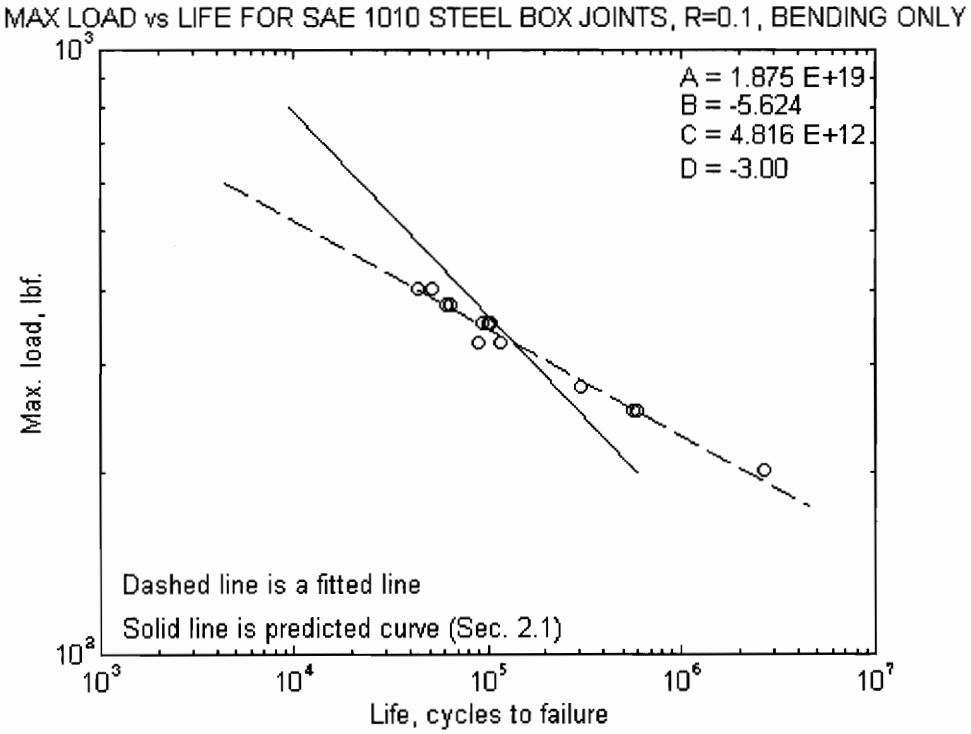

FIGURE 3.20 - S-N type data for SAE 1010 steel box joints, R=0.1, Bending only mode

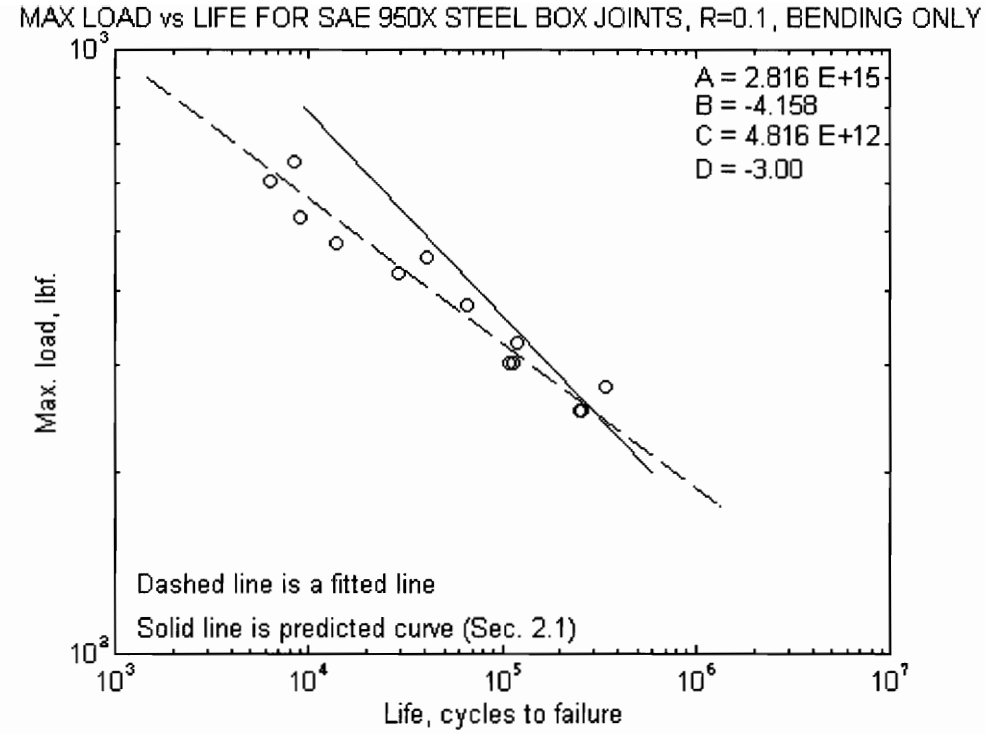

FIGURE 3.21 - S-N type data for SAE 950X steel box joints, R=0.1, Bending only mode

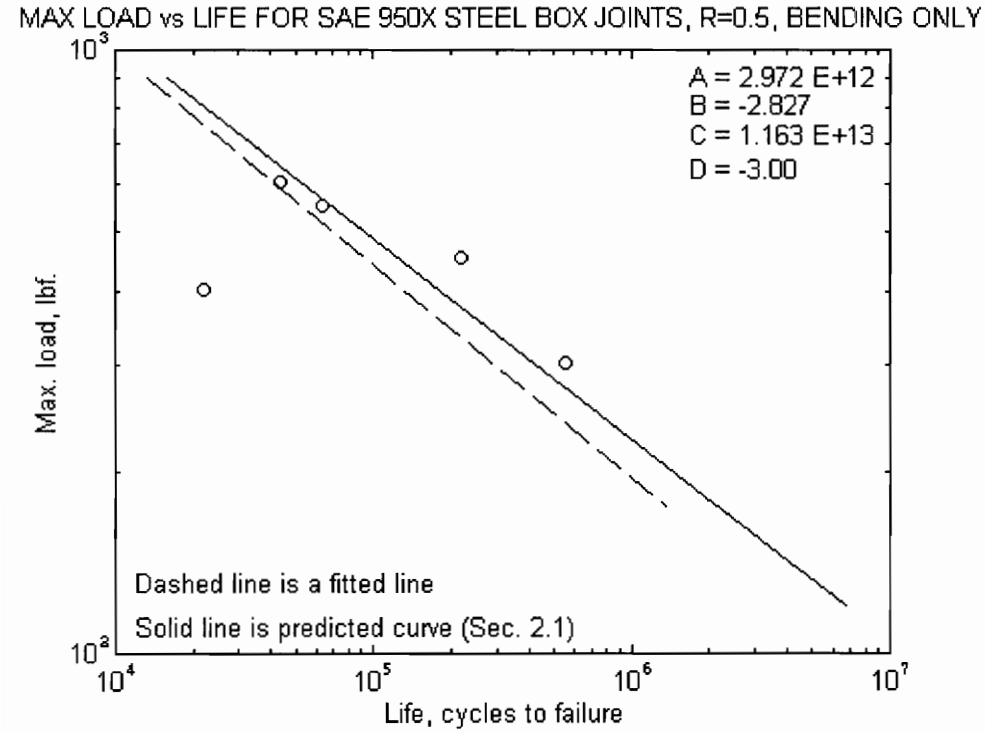

FIGURE 3.22 - S-N type data for SAE 950X steel box joints, R=0.5, Bending only mode

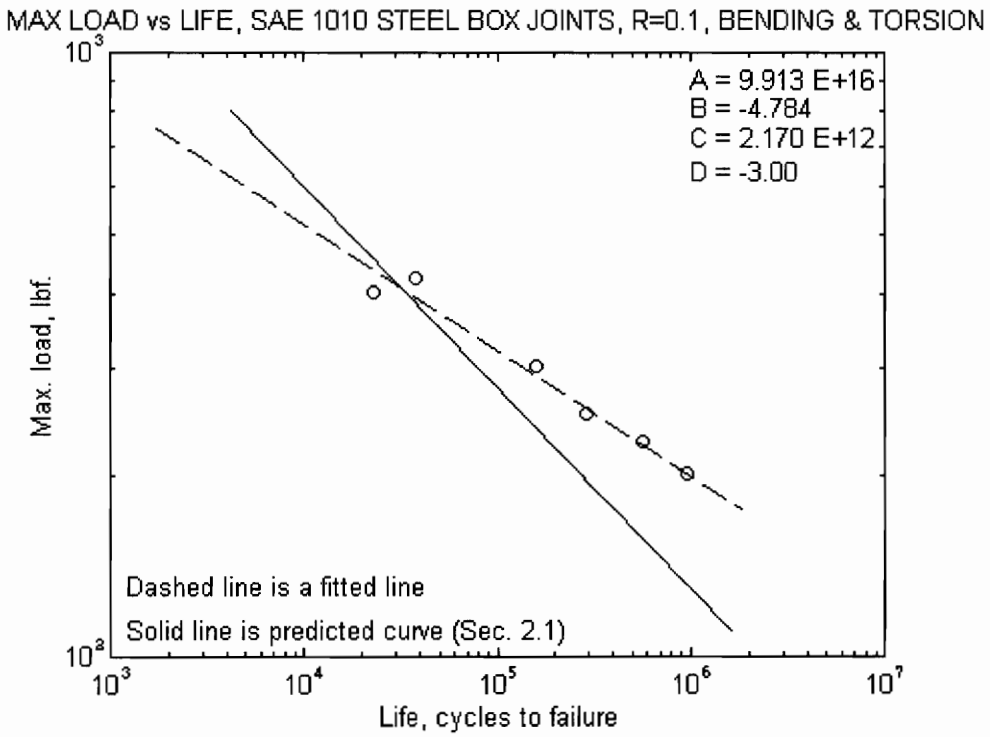

FIGURE 3.23 - S-N type data for SAE 1010 steel box joints, R=0.1, Bending and Torsion mode

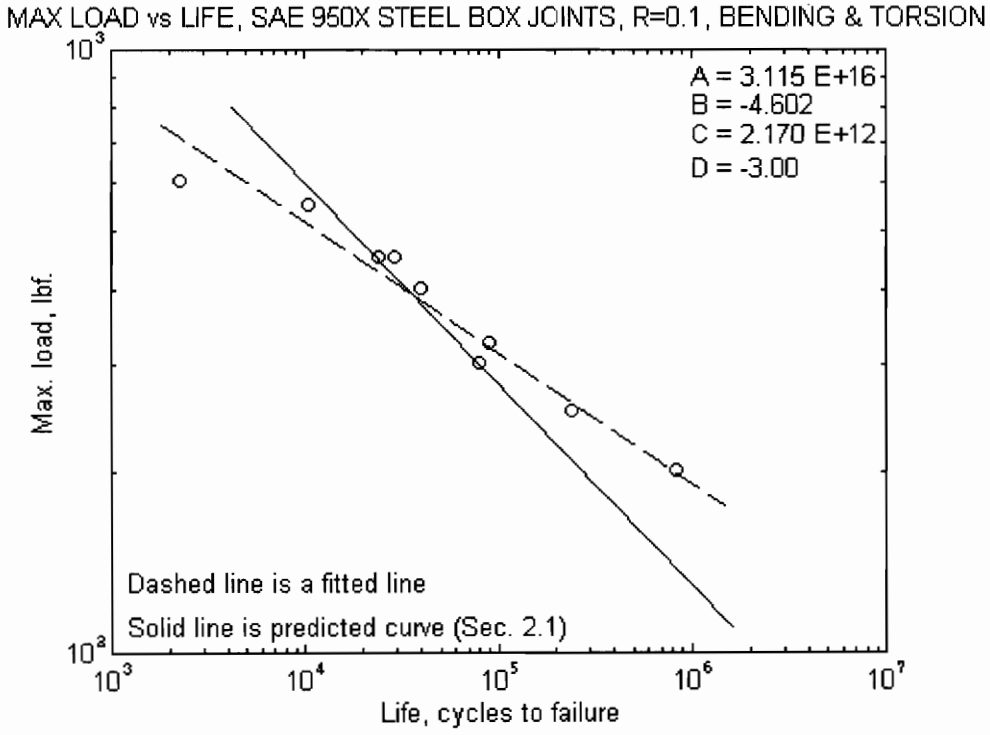

FIGURE 3.24 - S-N type data for SAE 950X steel box joints, R=0.1, Bending and Torsion mode

4. DISCUSSION

From the load-life plots shown in Chapter 3, it can be seen that the lives of peel joints were not accurately predicted. The slopes of the predicted lines and the fitted lines were fairly close in the case of peel joints. For this reason this discussion is largely limited to lap joints and to some extent box joints.

Predictions made for lap joints were close to actual data for a wide range of lives. In light of the assumptions made while developing the model(s) it may be remarkable that such accuracy is attainable. Another observation that can be made from the data is load-life behavior seems independent of the type of steel used. Plotted on the same plot, all data seems to fall along a single line. Furthermore, because Walker's equation was used in the life predictions it is possible to condense all lap joint data to a single plot. Strictly speaking Walker's equation allows an effective zero-to-mean stress intensity range which is defined as: [45]

$$\overline{\Delta K} = \frac{\Delta K}{(1-R)^{(1-\gamma)}} \tag{4.1}$$

Since the stress intensity range is a linearly related to the applied load range, an effective zero-to-max load, $\overline{P^{max}}$, can be defined as:

$$\overline{P^{max}} = \frac{P^{max}}{(1-R)^{-\gamma}} \tag{4.2}$$

Now a single plot can be made that encompasses all of the lap joint data and a single predicted line can be plotted along with the data. This effective zero-to-max load-life plot is given as Figure 4.1 for $\gamma = 0.5$. The constants that fit Eqs. 3.1 and 3.2 are displayed in the upper right corner of the plot. Different symbols exist for each of the distinct load ratios, R. They are as follows: o =>R=0.1, * =>R=0.5, + =>R=0.75.

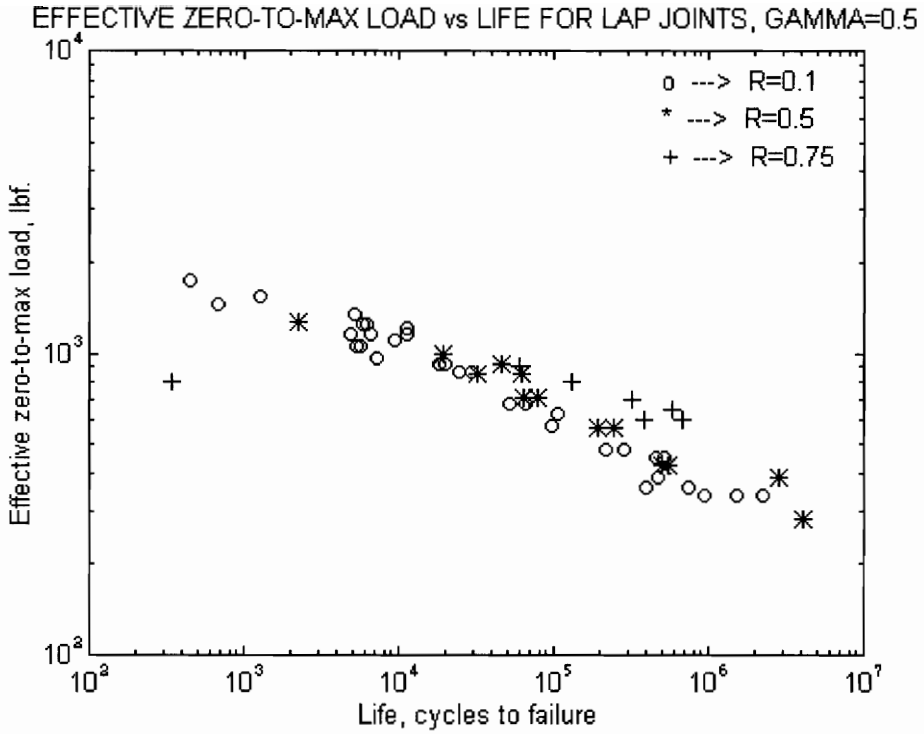

FIGURE 4.1 - Effective zero-to-max load versus life for lap joints, $\gamma = 0.5$

The choice of $\gamma = 0.5$ was made because this is a typical value for the base metals used to construct the specimens. Results for other values of γ have been examined also. Similar to Figure 4.1, Figures 4.2 and 4.3 show how the lap joint data collapses for $\gamma = 0.25$ and $\gamma = 0.75$, respectively. This has been done to test the sensitivity of γ . As can be seen from Figures 4.2 and 4.3, the choice of $\gamma = 0.25$ does not collapse the data as close as $\gamma = 0.5$. The data seems to collapse nicely for $\gamma = 0.75$, even more so than $\gamma = 0.5$. It is difficult to state with confidence what the true value of γ is, but it seems to be at least as great as 0.5. The changes in the three figures (4.1, 4.2, and 4.3) indicate that a small change inγ does not greatly change the quality of the collapsed curve. Ballpark estimates of γ will ensure accurate life prediction because the results are not extremely sensitive to its specific value.

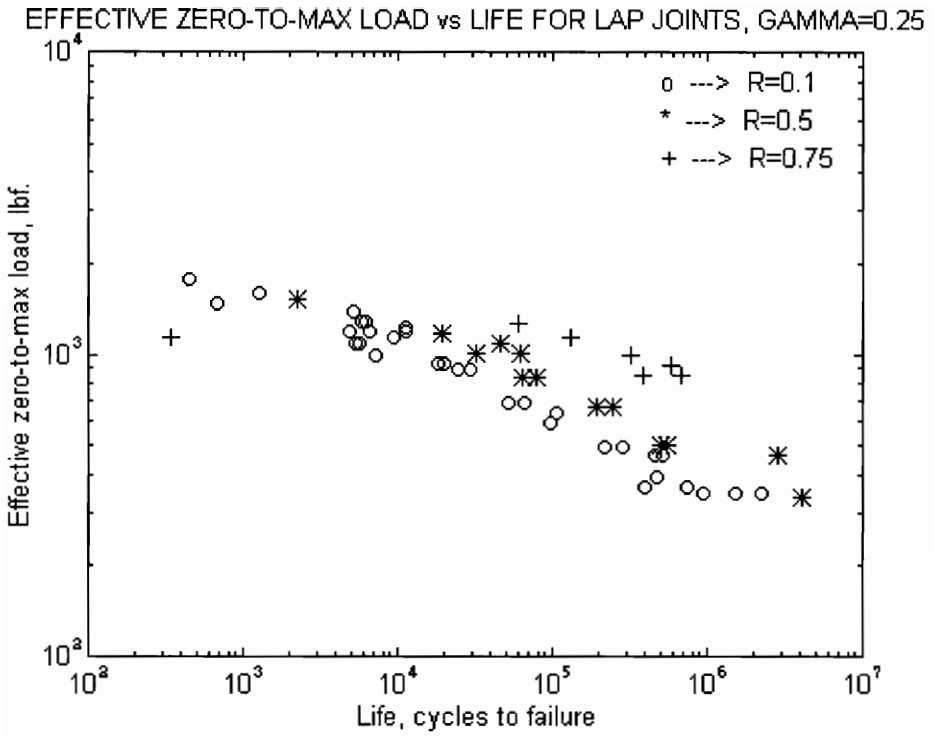

FIGURE 4.2 - Effective zero-to-max load versus life for lap joints, $\gamma = 0.25$

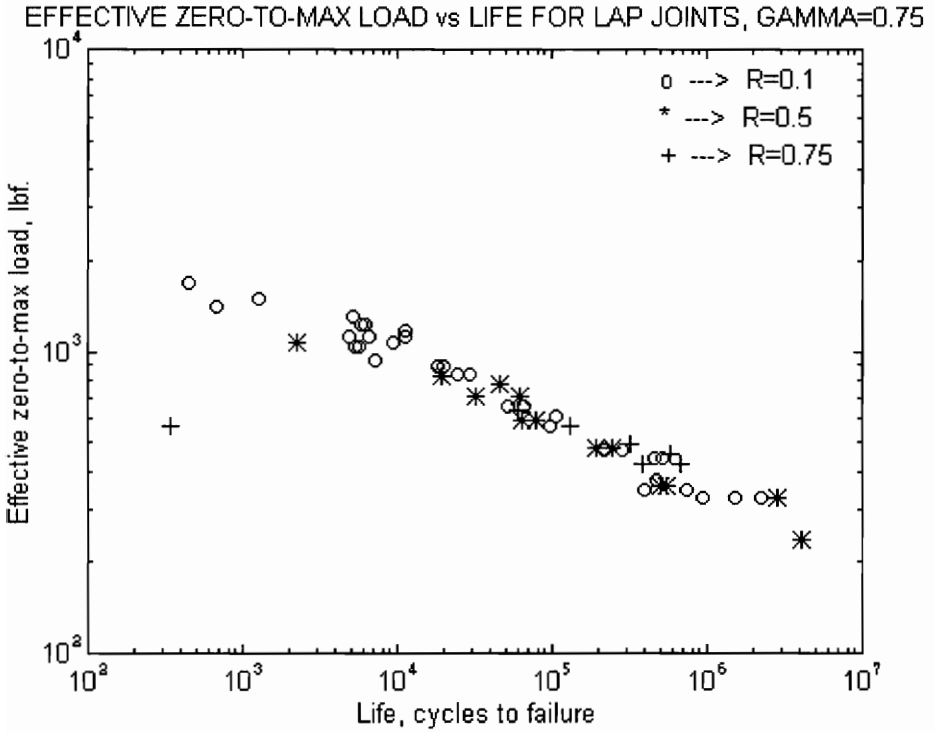

FIGURE 4.3 - Effective zero-to-max load versus life for lap joints, $\gamma = 0.75$

The sensitivity of the value of C, another constant of Walker's equation has also been examined. Acceptable ranges for C were obtained from a book by J. M. Barsom. [46] The value of C used in this paper, $C = 1.0 * 10^{-9}$, was found to be typical for the steels used to construct the test specimens. Two other values of C, $C = 1.0 * 10^{-8}$ and $C = 1.0 * 10^{-10}$, were also used to formulate predicted curves and plotted along with the data as generated in Figure 4.1 ($\gamma = 0.5$). These three predicted curves are shown in Figure 4.4. It can be seen that the value of C seems to demonstrate a greater degree of sensitivity than did γ. Because the accepted range of C varies greatly. The specific value chosen could greatly effect the success of a predicted curve. Almost all of the data falls within the accepted band that theory predicted. It is worthy to note, as load is increased (or life decreased) the data falls shorter and shorter of the middle of the accepted band. Perhaps plasticity effects is the cause of this phenomenon.

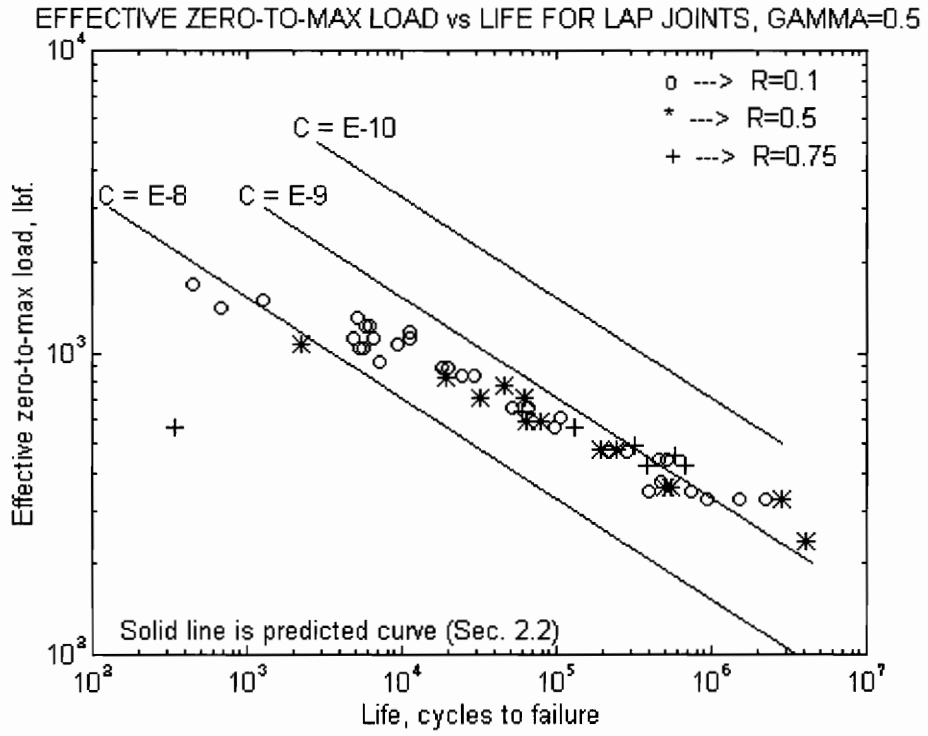

FIGURE 4.3 - Effective zero-to-max load versus life for lap joints, variable C

The sensitivity of geometric properties, such as sheet thickness, t, and weld radius, r, must be examined by looking at Eqs. 1.15 a-c. No experimental trends can be observed because each specimen provided by Ford Motor Company had the same sheet thickness and weld radius. Examination of the stress intensity equations (Eqs. 1.15 a-c), and how they apply to lap joints reveals that as the weld radius increases, the stress intensities are greatly reduced, thus increasing life. As the sheet thickness increases, the stress intensities are also reduced somewhat, and the specimen life is also extended. The stress intensity factors are more sensitive to changes in the weld radius, r, than to the sheet thickness, t.

The assumption that the stress intensity factor remains nearly constant as the crack grows may seem disturbing. This assumption was made with the understanding that the weld radius, r, is much greater than the sheet thickness, t. This is expressed mathematically as $r >> t$. (Note that Figure 2.1 is not drawn to scale.) Figure 4.5 is a sketch of a spot-weld as seen from the side, drawn approximately to scale. Note that the small growing crack, a, never grows to a significant size, compared to the weld radius. For all spot-welds tested here, $\frac{r}{t} \approx 3.5$. If a crack were to grow into the weld in the direction of a', as seen in Figure 4.5, then it would be reasonable to assume that the stress intensity factor(s) for this situation would be nearly constant for small a'. Or in the language of mathematical symbols, if $(r - a') \approx r$, then $K(r - a') \approx K(r)$.

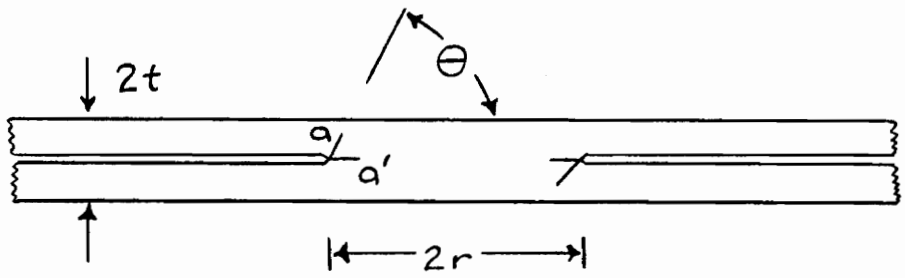

FIGURE 4.5 - Side view of spot-weld drawn to scale.

Strictly speaking, this is not the case because the crack propagates into the sheet metal at an angle. However, because the actual crack, a, is small, the fact that it grows at an angle should not greatly affect the stress intensity factor(s) given that the angle, Θ, is included in the analysis. However an approximation does certainly exist due to the finite size of the crack, a, especially as the crack approaches the outer surface, but this situation is mitigated to an extent, in this case, as the crack shape is nearly semi-elliptical, and the crack front does not extend infinitely in the third dimension.

Also it should be noted that the predicted lives obtained were done so without prior knowledge of the actual lives of the test data. The constants for Walker's equation could have been chosen so they best fit the data, but this was not done here.

5. CONCLUSION

This chapter is a discussion of the results of the two life prediction methods developed in this paper. The assumptions used to develop the two life prediction methods are restated and the assumptions thought to be the most questionable are discussed.

Many assumptions had to be made to make life prediction of spot-welds a manageable task. The simplifying assumptions used are as follows:

- The weld is circular and acts as a sharp crack.
- The rate of crack growth through the sheet metal is constant.
- The Walker equation applies and C, m, and γ are constant.
- The three dimensional problem can be approximated by a two dimensional model if the sheet metal thickness is small compared to the weld diameter. Furthermore, at the location of failure $K_{III} = 0$.
- The angle that the crack grows, Θ_o, remains constant for the life of the weld.
- The stress field at the crack tip is not changed much by the small kinked crack growing out of the original crack tip.
- The stress intensities given in Equations 1.15 a-c adequately represent the original stress intensity factors. This means the contribution of torsion, bending, and normal forces to the stress intensity factors are not dependent on the finite thickness of the sheet metal, and the average stress on the weld nugget does not exceed 80% of the yield stress.
- The specimen is sufficiently wide such that width effects are negligible.
- Residual stresses, although present, are assumed to be small and negligible.
- Failure occurs when a crack grows through a metal sheet to the outer surface.
- The thicknesses of both sheets of metal joined by any spot-weld are the same.
- Crack growth begins from the first cycle.

The lives predicted for peel joints were unacceptable. No numerical solution for stress intensity factors exist for finite peel geometries, and this is the probable cause of the poor results obtained for peel joints. The method for predicting lives appears to work for other geometries, so it is assumed that improvements could be made to these methods that would generate acceptable results.

Accurate stress intensity factors are known for finite lap joint geometries, and thus life prediction of lap joints was reasonably accurate. The error in predicting the lives of lap joints was small, which indicates that the assumptions made were not too severe (at least for the geometry and materials given).

Since the critical spot-welds were loaded in a manner similar to that of lap joints (See Table B.1), it is not surprising that the success of the life prediction methods was similar to that of lap joints. Because lap joints are considered to be more important structurally, and have received the most attention in the related literature, the work done here would be useful in most structural applications.

To summarize, the life prediction results:

- Life prediction for peel joints was not accurate
- The lives of lap joints were predicted well.
- Box joints behaved as lap joints because the critical spot-welds were loaded as a lap joint.

6. RECOMMENDATIONS

Although the methods developed here to predict the lives of spot-welds were not entirely successful, they still offered some reasonable results in the case of lap joints. It is suspected that improvements in a few key areas would greatly improve the results obtained by these methods. Listed below are what is thought to be the best ways to improve these already developed life-prediction methods. Short of a full blown numerical scheme, which may be practical in the near future, these suggestions offer the best chances of improving the existing life prediction methods.

- Find constants, which are used in the Walker equation, that are better suited for the HAZ. Constants have been used in this paper that are common for the base metals.

- Numerically solve for stress intensities that occur in finite geometries due to normal forces, bending moments, and torsion. L. P. Pook has already done this for shear forces. It is believed that new stress intensity factors would eliminate the need for Section 2.2.

- Examine the role of plasticity about the weld and how it affects the life of a spot-weld. This may explain why predicted lives tend to be non-conservative at high loads (for lap joints). [47]

- Include residual stresses.

- Consider deflections of the weld and how they will change the loading as seen by the spot-weld.

7. REFERENCES

[1] **Overbeeke, J.L.** and **J. Draisma**, (1974), "Fatigue Characteristics of Heavy Duty Spot-welded Lap Joints," *Metal Construction and British Welding Journal*, July 1974, pp 213-219.

[2] **Davidson, J.A.** and **E.J. Imhof**, (1984), "The Effect of Tensile Strength on the Fatigue Life of Spot-welded Sheet Steels," SAE paper 840110, Soc. Auto. Engrs., Warrendale, PA.

[3] **Orts, D.H.**, (1981), "Fatigue Strength of Spot Welded Joints in a HSLA Steel," SAE paper 810355, Soc. Auto. Engrs., Warrendale, PA.

[4] **Mizui, M.**, etc., (1988), "An Evaluation of Fatigue Strength for Various Kinds of Spot-welded Test Specimens," SAE paper 880375, Soc. Auto. Engrs., Warrendale, PA.

[5] **McMahaon, J.C., G.A. Smith**, and **F.V. Lawrence**, (1990), "Fatigue Crack Initiation and Growth in Tensile-Shear Spot Weldments," *Fatigue and Fracture Testing of Weldments*, ASTM STP 1058, H.I. McHenry and J.M. Potter, Eds., American Society for Testing and Materials, Philadelphia, pp. 47-77.

[6] **Lawrence, F.V., P. C. Wang**, and **H.T. Corten**, (1983), "An Empirical Method for Estimating the Fatigue Resistance of Tensile-Shear Spot-welds," SAE paper 830035, Soc. Auto. Engrs., Warrendale, PA.

[7] **Lawrence, F.V., R. Mattos, Y. Higashida**, and **J. Burk**, (1978), "Estimation of Fatigue Crack Initiation Life of Weld," ASTM STP 648, p.134, American Society of Testing and Materials, Philadelphia, PA.

[8] **Kan, Y.**, (1976), "Fatigue Resistance of Spot-welds--An analytical Study," *Metals Engineering*, Nov. 1976, pp. 26-36.

[9] **Sheppard, S.D.** and **M. Strange**, (1992), "Fatigue Life Estimations in Resistance Spot Welds: Initiation and Early Growth Phase," *Fatigue and Fracture of Engineering Materials and Structures*, Vol. 15, No. 6, pp. 531-549.

[10] **Cooper, J. F.** and **R. A. Smith,** (1986), "Fatigue crack propagation at spot welds," *Metal Construction*, June 1986, pp. 383-386.

[11] **Overbeeke, J.L.** and **J. Draisma**, (1978), "Influence of Stress Relieving on Fatigue of Heavy Duty Spot Welded Lap Joints," *Metal Construction*, September 1978, pp. 433-434.

[12] **Pook, L.P.,** "Approximate stress intensity factors for spot and similar welds," NEL Report 588 (National Engineering Laboratory, UK, 1975).

[13] **Sheppard, S.D.**, (1993), "Estimation of Fatigue Propagation Life in Resistance Spot Welds," *Advances in Fatigue Lifetime Predictive Techniques: Second Volume*, ASTM STP 1211, M.R. Mitchell and R.W. Landgraf, eds., American Society for Testing and Materials, Philadelphia, PA.

[14] **Kurath, P.**, (1992), "Multi-axial Fatigue Criteria for Spot Welds," SAE paper 920668, Soc. Auto. Engrs., Warrendale, PA.

[15] **VandenBossche, D.J.**, (1977), "Ultimate Strength and Failure Mode of Spot Welds in High Strength Steels," SAE paper 770214, Soc. Auto. Engrs., Warrendale, PA.

[16] **Sperle, J-O.**, (1983), "Strength of Spot Welds in High Strength Steel Sheet," *Metal Construction*, April 1983, pp. 200-203.

[17] **Pollard, B.**, (1974), "Spot Welding Characteristics of HSLA Steel for Automotive Applications," *Metal Construction*, August 1974, pp. 343-350.

[18] **Wang, T.J.**, (1994), "Damage analysis of low alloy steel (15MnMoVNRe) and its simulated coarse-grained heat affected zone," *Theoretical and Applied Fracture Mechanics* v. 21, pp. 23-28.

[19] **Wang, T.J.**,(1991), "A continuum damage model for ductile fracture of weld heat affected zone," *Engineering Fracture Mechanics*, v. 40, pp. 1075-1082.

[20] **Wang, T.J.** and **Z. Lou**, (1990), "A continuum damage model for weld heat affected zone under low cycle fatigue loading," *Engineering Fracture Mechanics*, v. 37, pp. 825-829.

[21] **Davidson, J.A.** and **E.J. Imhof**, (1983), "A Fracture-Mechanics and System-Stiffness Approach to Fatigue Performance of Spot-welded Sheet Steels," SAE paper 830034, Soc. Auto. Engrs., Warrendale, PA.

[22] **Davidson, J.A.**, (1983), "A Review of the Fatigue Properties of Spot-welded Sheet Steels," SAE paper 830033, Soc. Auto. Engrs., Warrendale, PA.

[23] **Pook, L.P.**, (1975), "Fracture Mechanics Analysis of the Fatigue Behavior of Spot Welds," *International Journal of Fracture*, v. 11, pp. 173-176.

[24] **Landgraf, R.W.**, personal conversations with, Professor of Engineering Science and Mechanics, Virginia Polytechnic Institute and State University

[25] **Lawrence, F.V.** and **J.-Y. Yung**, (1986), "Estimating the Effects of Residual Stress on the Fatigue Life of Notched Components".

[26] **Wang, P.C.**, **H.T. Corten**, and **F.V. Lawrence**, (1985), "A Fatigue Life Prediction Method for Tensile-Shear Spot Welds," SAE paper 850370, Soc. Auto. Engrs., Warrendale, PA.

[27] **Mabuchi, A.**, **J. Nilsawa**, and **N. Tomioka**, (1986),"Fatigue Life Prediction of Spot-Welded Box-Section Beams under Repeated Torsion," SAE paper 860603, Soc. Auto. Engrs., Warrendale, PA.

[28] **Kitagawa, H.**, **T. Satoh**, and **Fujimoto**, (1985), "Fatigue Strength of Single Spot-Welded Joints of Rephosphorized High-Strength and Low-Carbon Steel Sheets," SAE paper 850371, Soc. Auto. Engrs., Warrendale, PA.

[29] **Lawrence, F.V.** et al., (1981),"Predicting the Fatigue Resistance of Welds," *Annual Review of Material Science*, v. 11, pp. 401-425.

[30] **Weixing, Y.** et al., (1995),"On the fatigue notch factor, K_F," *International Journal of Fatigue*, v. 17, No. 4, pp. 245-251.

[31] **Peterson , R. E.,** "Notch-Sensitivity," *Metal Fatigue*, G. Sines and J. L. Waisman, Eds., 1959.

[32] **Swellam, M.H., P. Kurath**, and **F.V. Lawrence**, (1992), "Electric-Potential-Drop Studies of Fatigue Crack Development in Tensile-Shear Spot Welds," *Advances in Fatigue Lifetime Predictive Techniques*, ASTM STP 1122, M.R. Mitchell and R.W. Landgraf, Eds., American Society for Testing and Materials, Philadelphia, pp. 383-401.

[33] **Cooper, J.F.** and **R.A. Smith**, (1985), "The Measurement of Fatigue Cracks at Spot-welds," *International Journal of Fatigue*, July 1985, pp. 137-140.

[34] **Barsom, J.M., J.A. Davidson**, and **E.J. Imhof**, (1985), "Fatigue Behavior of Spot Welds under Variable-Amplitude Loading," SAE paper 850369, Soc. Auto. Engrs., Warrendale, PA.

[35] **Matsoukas, G., P. Steven**, and **Y. W. Mai**, (1984), "Fatigue of spot-welded lap joints," *International Journal of Fatigue*, v. 6, No. 1, January 1984, pp. 55-57.

[36] **Shinozaki, M., T. Kato, I. Takahaski**, and **T. Irie**, (1983), "Fatigue of Automobile High Strength Steel Sheets and Their Welded Joints," SAE paper 830032, Soc. Auto. Engrs., Warrendale, PA.

[37] **Pollard, B.**, (1982), "Fatigue Strength of Spot Welds in Titanium-Bearing HSLA Steels," SAE paper 820284, Soc. Auto. Engrs., Warrendale, PA.

[38] **Paris, P.C.** and **F. Erdogan**, (1963), "A critical Analysis of Crack Propagation Laws," Transactions of the ASME, *Journal of Basic Engineering*, Series D, 85, No.3.

[39] **Tanaka, K.**, (1974), "Fatigue Crack Propagation from a crack inclined to the Cyclic Tensile Axis," *Engineering Fracture Mechanics*, v. 6, pp. 493-507.

[40] **Iida, S.** and **A.S. Kobayashi**, (1969), "Crack propagation rate in 7075-T6 plates under cyclic tensile and transverse shear loading," *Journal of Basic Engineering*, ASME 91, pp. 764-769.

[41] **Erdogan, F.** and **G.C. Sih**, (1963), "On the Crack Extension in Plats under Plane Loading and Transverse Shear," *Journal of Basic Engineering*, ASME 85, pp.519-527.

[42] **Smith, C.W.**, personal conversations with, Professor of Engineering Science and Mechanics, Virginia Polytechnic Institute and State University.

[43] **Overbeeke, J.L.**, (1976), "Fatigue of Spot Welded Lap Joints," *Metal Construction*, May 1976, pp. 212- 215.

[44] **Bolton, W.**, (1961), "Residual Stress Distribution in and around Spot Welds," *British Welding Journal*, Feb. 1961, p.576-579.

[45] **Dowling, N. E.**, (1993), *Mechanical Behavior of Materials*, Prentice Hall, 1993.

[46] **Barsom, J. M.**, (1987), *Fracture & Fatigue Control in Structures*, 2nd Ed., Prentice Hall, 1987.

[47] **Dowling, N. E.**, (1976), "Geometry Effects and the J-Integral Approach to Elastic-Plastic Fatigue Crack Growth," *Cracks and Fracture*, ASTM STP 601, 1976.

APPENDIX A. TEST FIXTURE DETAILS

This Appendix includes detailed information about the box joint test fixture that is not entirely needed to appreciate this report. This fixture is symmetric, with the exception of bending and torsion loading, when spacers are the only components that are not symmetric. The fixed ends of a box joint specimen (Figure 3.16, page 40) are bolted to the web of an 8 inch deep I-beam. Spacers are used to insure a proper fit. The I-beam is bolted to an aluminum collar which clamps around the posts of an MTS machine. These collars are 4 inches thick and are called upper collars. See Figure A.1 for a sketch of an upper collar. Note that both upper collars are made identical.

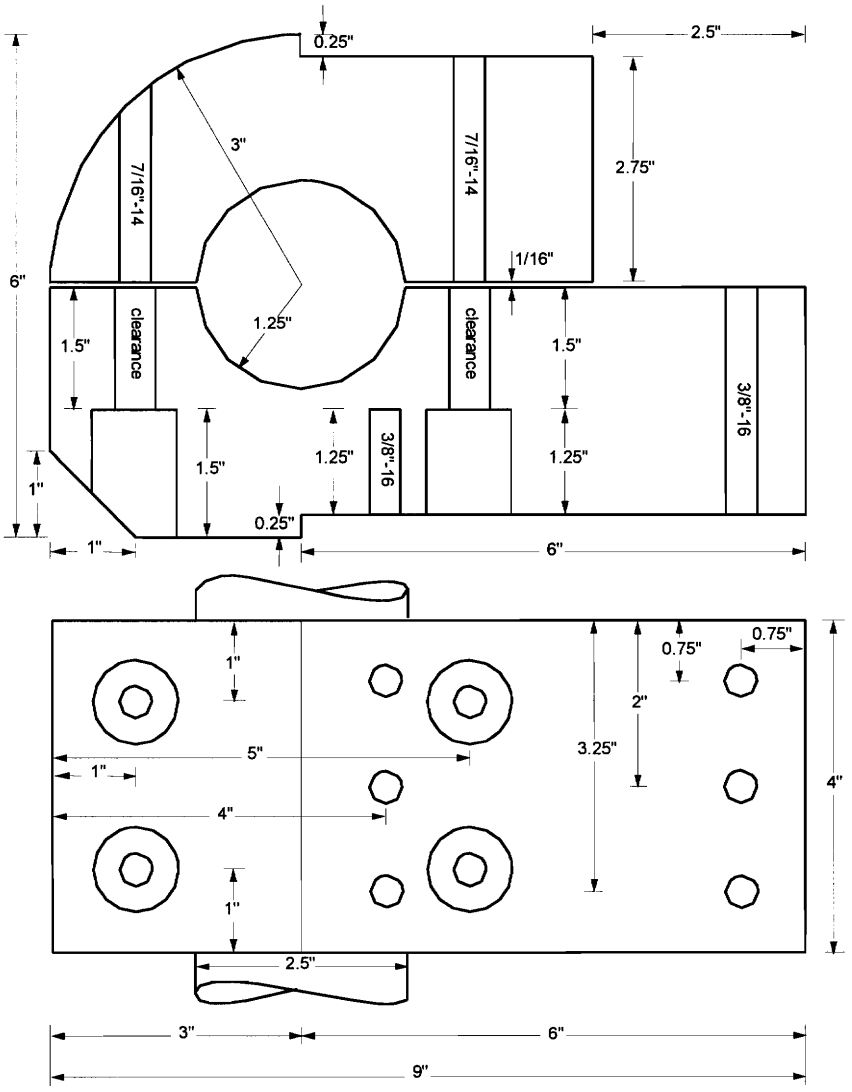

FIGURE A.1. Sketch of an upper collar of box joint test fixture. Upper sketch is a top view, while the bottom is a side view.

The two pieces of an upper collar are clamped together with four 7/16"-14 bolts. With the exception of these bolts, all others are 3/8"-16 threaded bolts. For the bending only case, the I-beams are on the inside closest to each other. Bending and torsion loading requires the I-beams be moved to the outside furthest from each other. Each I-beam is bolted to an upper collar with six bolts. The bolts holding the I-beam are not quite strong enough to safely support the structure under the most severe loading. The factor of safety is nearly 1. For this reason, braces on each I-beam were created. The braces are made of 3" deep channel. The braces are bolted to the web of an I-beam on one end and to another collar on the other end. The flange of each I-beam had to be cut away along part of the bottom to accommodate this arrangement. These other collars are only 3" thick and are called lower collars. See Figure A.2 for a sketch of a lower collar. Both lower collars are also made identical. Figure A.3 is a sketch of the side of the entire structure as discussed so far.

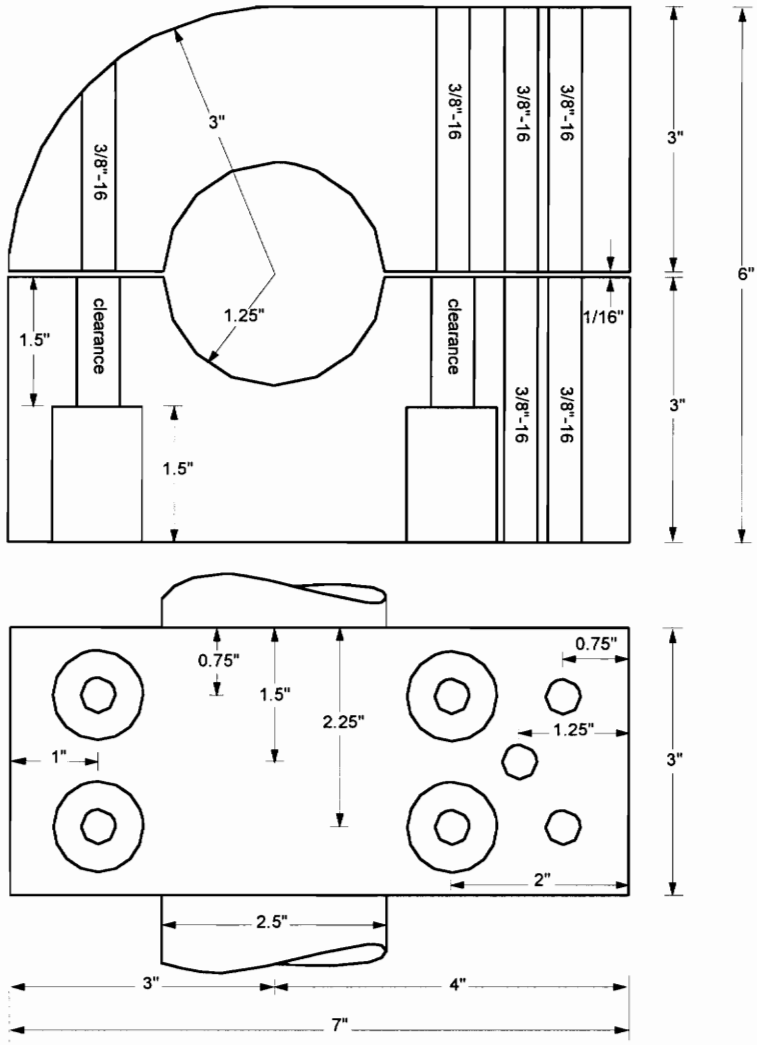

FIGURE A.2. Sketch of a lower collar of box joint test fixture. Upper sketch is a top view, while the bottom is a side view.

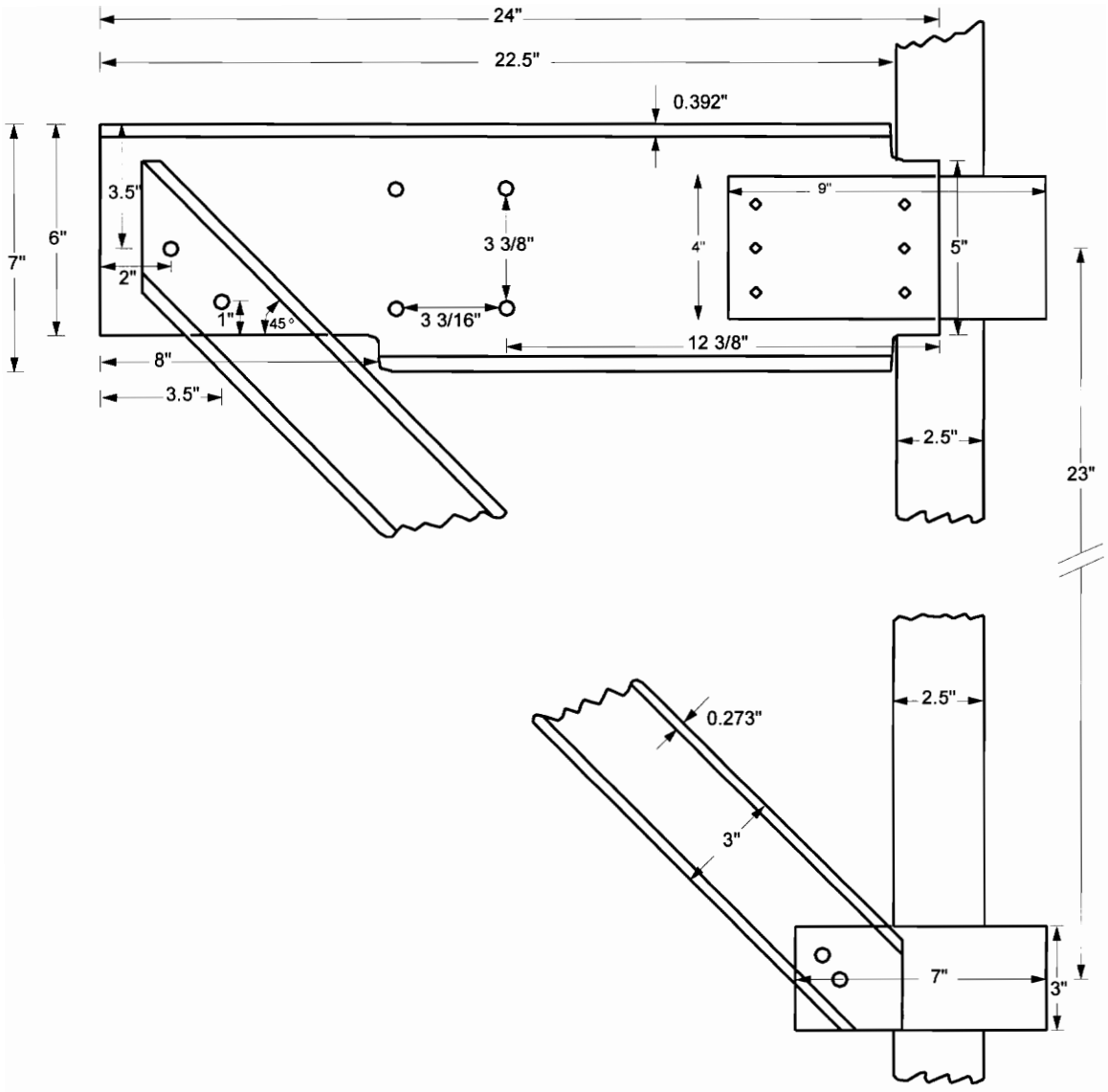

FIGURE A.3. Sketch of test fixture as seen from the side.
(Note that both MTS machine posts are in line.)

The spacers that were discussed previously are shown in Figure A.4, with the exception of one spacer used only in the bending and torsion setup. Because it was unusually long, over 13 inches, this particular spacer was made out of 1.5" thick aluminum sheet metal and constructed like an I-beam. It is called the long spacer. All other spacers, shown in Figure A.4, are described by spacer thickness.

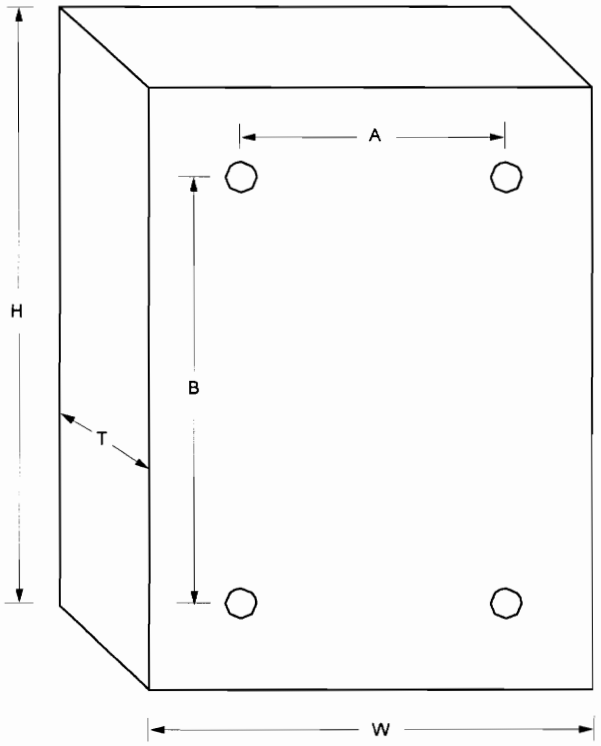

Quantity	A	B	H	W	T
2	3 3/16"	3 3/8"	5"	4"	1/8"
2	3 3/16"	3 3/8"	5"	4"	1 7/8"
1	3 3/16"	3 3/8"	5"	4"	1 9/16"
1	3 3/16"	3 3/8"	5"	4"	1 5/16"
1	3 3/8"	4 3/16"	5 1/4"	5"	1/18"

FIGURE A.4. Diagram of spacer geometry, tables of quantities and dimensions of each.

As shown in Figure 3.16, a piece must attach to the front plate of the box joint. Cantilevers protruding from a steel plate bolted to the specimen was a design suggested by the sponsor. This suggestion was used in our design. For the bending only case, a 3/4" steel rod as a cantilever was found to be sufficient. It was placed in a hole in the center of the steel plate and welded. The bending and torsion loading required an "L" shaped cantilever. A 2" square box beam was used with 3/4" steel rod protruding from one end. This was also placed in a hole in the steel plate and welded. These parts are called the straight cantilevered rod and bent cantilevered rod, respectively. See Figure A.5 for a sketch of both cantilevered rods.

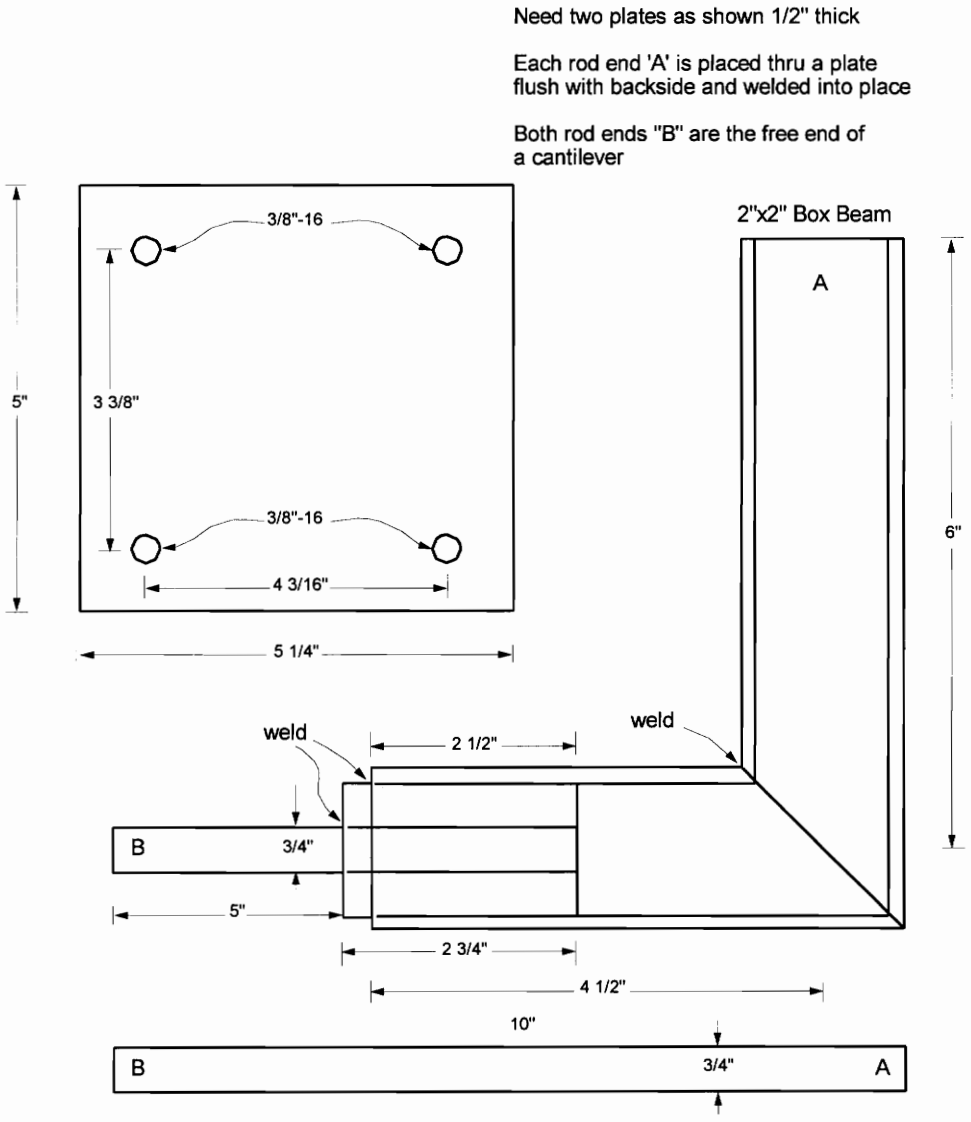

FIGURE A.5. Sketch of both cantilevered rods before assembly.

Since the load cell usually used by the MTS machine was excluded from the load path, a problem arose. A load cell was needed. An Interface load cell, rated at 5000 lbf., was purchased from an MTS Direct catalog. Connecting to the proper location on a cantilevered rod was tricky. As the box joint deflected, the loading point moved towards the specimen, creating a side load on the actuator and a component of force on the specimen normal to the cantilevered rod. To reduce these effects, a ball joint end was used to apply a force to the cantilevered rod. This ball joint end was screwed into a 2" diameter aluminum shaft. On the other end of the shaft, which was 12" long, was the load cell. On the other end of the load cell was a smaller piece of the 2" diameter aluminum shaft. The load cell was connected to the shafts by 2" long pieces of threaded rod. This entire assembly of aluminum shafts, load cell, and ball joint end was called the load cell assembly. Finally, a clevis, which was gripped in the lower grips of an MTS machine, was pinned to the smaller piece of aluminum shaft. The clevis was readily available and borrowed from Virginia Tech's Materials Testing Lab. See Figure A.6 for a sketch of the clevis, and Figure A.7 for a sketch of the load cell assembly without the load cell. This design kept the secondary effects of deflections as small as possible and kept the dynamic effects of a swinging load cell to a minimum. Sliding of the ball joint end on the cantilevered rod is assumed not to occur. Hose clamps are used to resist such sliding, and in the event of sliding, alert the test operator. No problems with sliding have arisen. Additional photos of the assembled test fixture are shown in Figures A.8 and A.9.

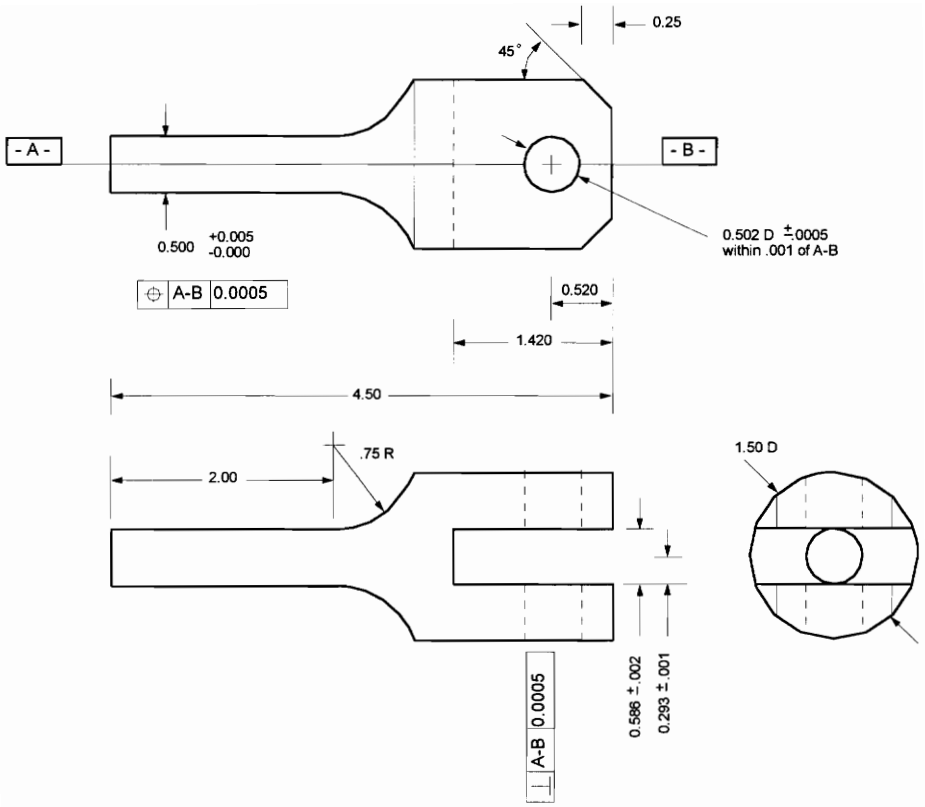

FIGURE A.6. Sketch of clevis.

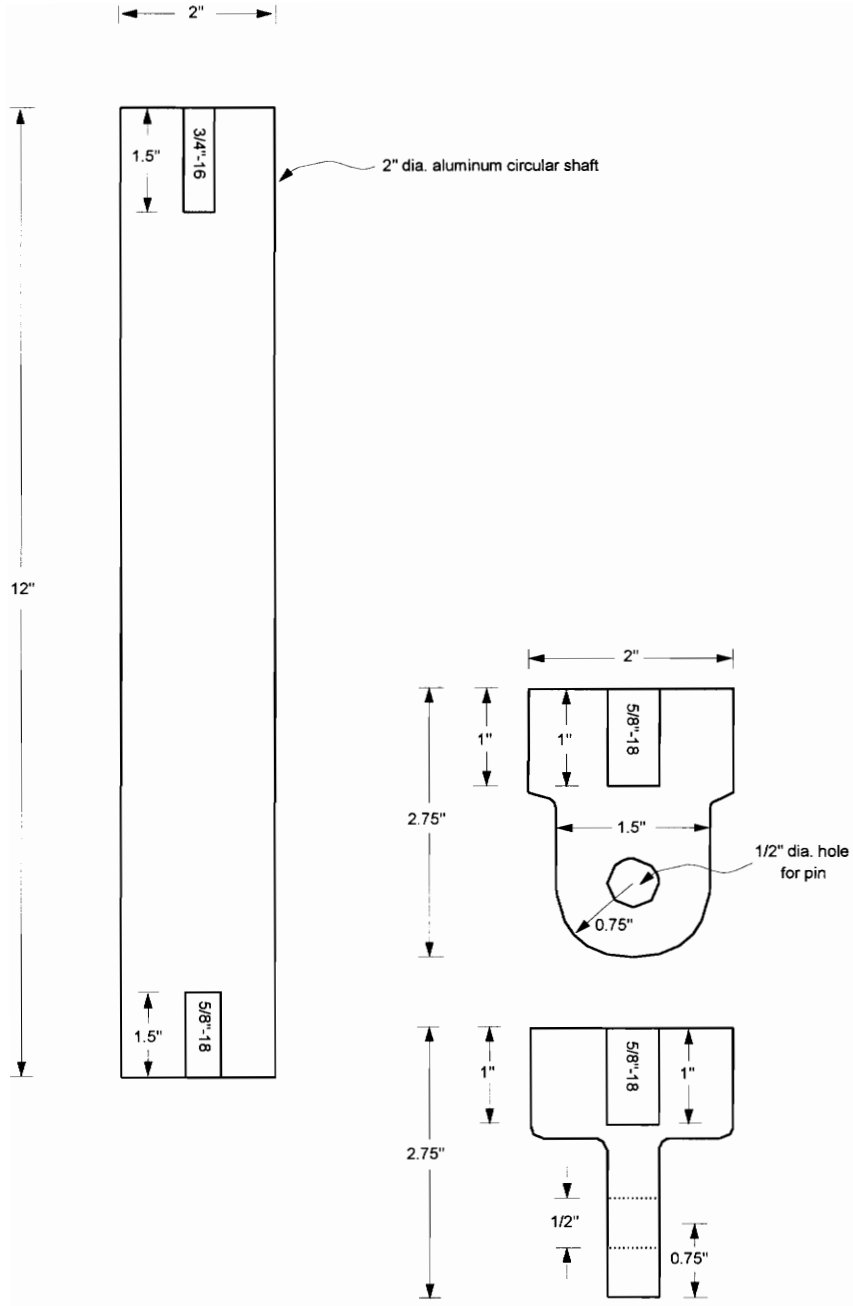

FIGURE A.7. Sketch of load cell assembly without the load cell.

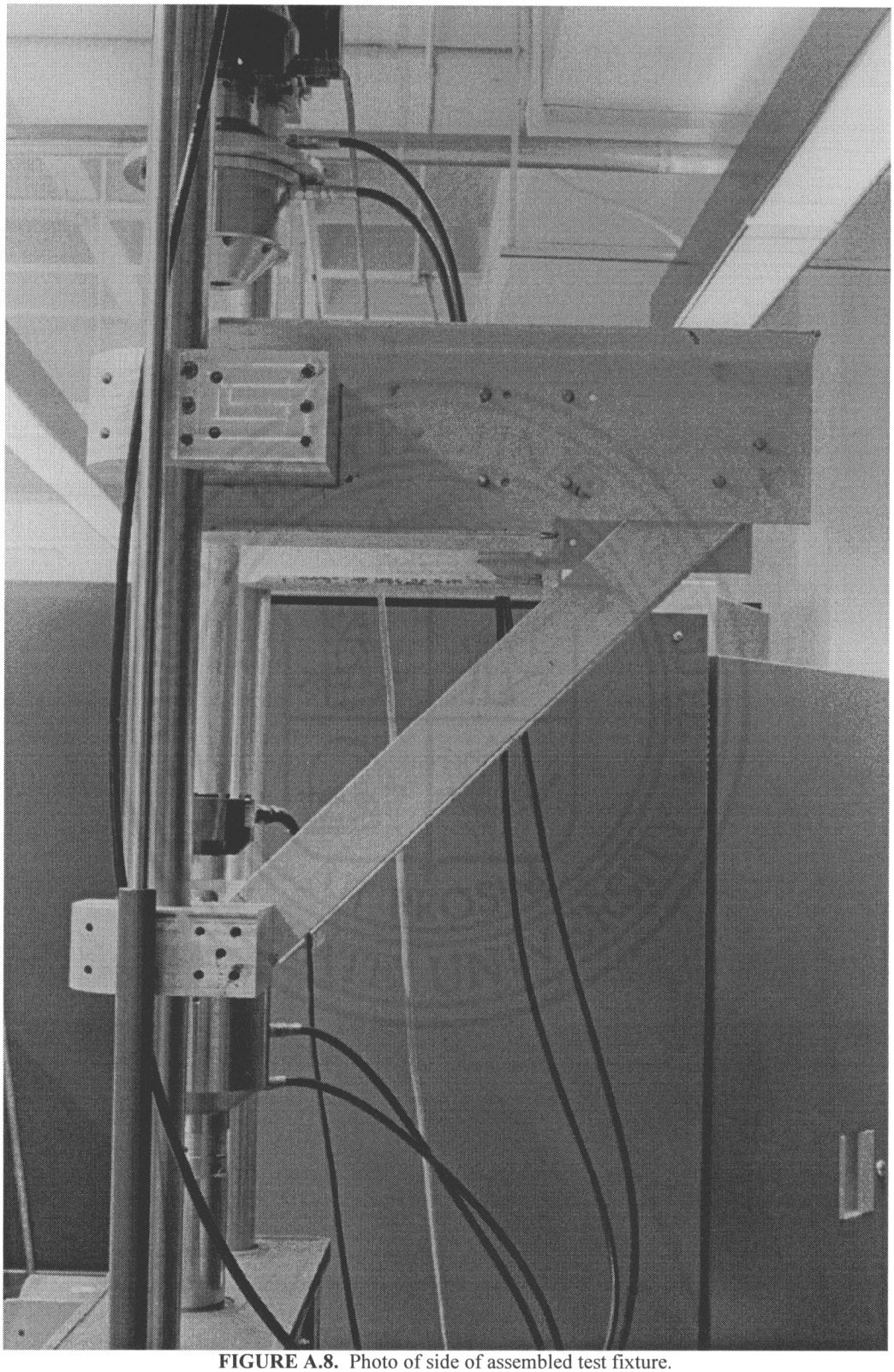

FIGURE A.8. Photo of side of assembled test fixture.

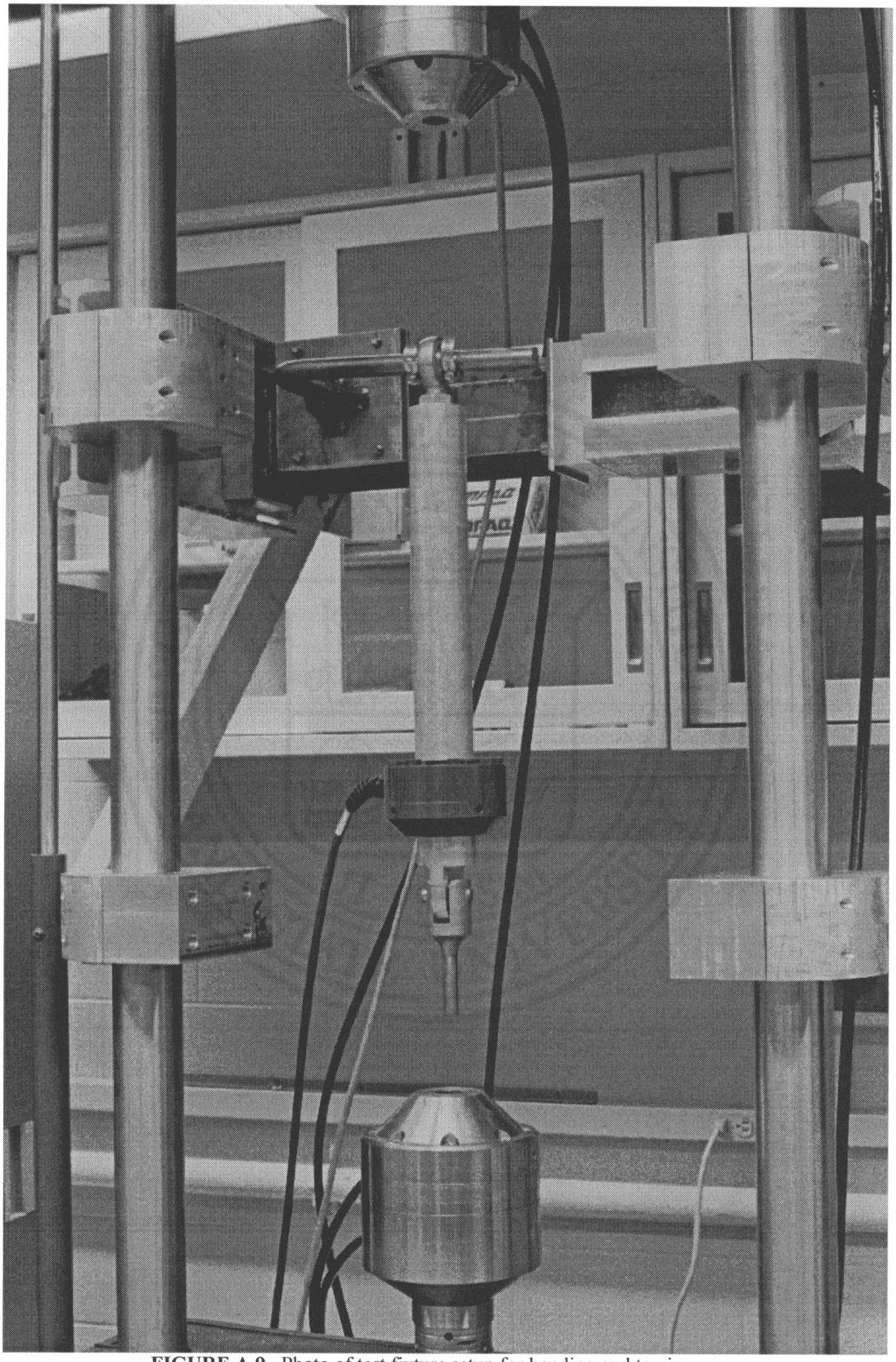

FIGURE A.9. Photo of test fixture setup for bending and torsion case.

APPENDIX B. FORTRAN CODES

The first program listed corresponds to the method of Section 2.1. The Newton-Raphson method is used to solve Eq. 2.5 for the angle of crack growth. This method was chosen because a derivative was easy to calculate and convergence is fast. A good initial value is key to rapid convergence. An initial value of 0.7 radians seems to work well for all of the cases tested, but not necessarily for all imaginable cases. Comments are included in the event that debugging or modification is needed in the future. The angular position of failure, F, used in the program is the angle ϕ seen in Chapters 1 and 2. This should be the position of maximum stress intensity, which coincides with the location of failure. For most geometries this would be zero. The information output is as follows:

(1) Effective stress intensity range, ΔK_I^{eff}

(2) Effective zero-to-max. stress intensity range, $\frac{\Delta K_I^{eff}}{(1-R)^{(1-\gamma)}}$

(3) Angle of crack growth, Θ_o

(4) Number of cycles to failure (surface crack), N_f

```
PROGRAM MAXOPEN

   REAL   F1,F2,F3,M1,M2,M3,A,T,C,M,G,R,F,TH
   REAL   K1,K2,K3,KE,NF,C1,C2,C3,DUM,N,KTH
   INTEGER I

******* INPUT OF LOADING, MATERIAL, AND GEOMETRIC INFORMATION *****

   WRITE(6,*)'   CONSTANT GROWTH / NO RESIDUAL STRESS'
   WRITE(6,*)'        LIFE PREDICTION MODEL '
   WRITE(6,*)
   WRITE(6,*)
   WRITE(6,*)'THIS PROGRAM ESTIMATES THE LIFE OF A SPOT-WELDED'
   WRITE(6,*)'CONNECTION BETWEEN TWO SHEETS OF STEEL.'
   WRITE(6,*)'THE ASSUMPTIONS MADE IN DEVELOPING THIS MODEL ARE'
   WRITE(6,*)'   1. NEGLIGIBLE RESIDUAL STRESSES'
   WRITE(6,*)'   2. CONSTANT MATERIAL PROPERTIES AT CRACK TIP'
   WRITE(6,*)'   3. FORCE AND MOMENT RESULTANTS ARE KNOWN'
   WRITE(6,*)'   4. FORCE AND MOMENT LOAD RATIOS ARE ALL'
   WRITE(6,*)'      IDENTICAL AND CONSTANT'
   WRITE(6,*)'   5. CRACK GROWTH IS CONSTANT'
   WRITE(6,*)'   6. CRACK GROWS IN PRINCIPAL STRESS DIRECTIONS'
   WRITE(6,*)'   7. ANGLE OF CRACK GROWTH IS CONSTANT'
   WRITE(6,*)'   8. EFFECTIVE STRESS INTENSITY IS RELATED TO'
   WRITE(6,*)'      THE ORIGINAL STRESS INTENSITIES'
   WRITE(6,*)'   9. CRACK REORIENTATION OCCURS AT THE MOMENT'
   WRITE(6,*)'      LOADING BEGINS.'
```

```
      WRITE(6,*)'   10. A THRESHOLD VALUE FOR STRESS INTESSITY FACTORS'
      WRITE(6,*)'       EXISTS BELOW WHICH CRACKS DO NOT PROPAGATE.'
      WRITE(6,*)
      WRITE(6,*)
      WRITE(6,*)'SEE FIGURES 1.1 AND 1.2 TO INPUT THE FOLLOWING DATA'
      WRITE(6,*)
      WRITE(6,*)
      WRITE(6,*)'INPUT THE SHEAR FORCE F1 (N).'
      READ *,F1
      WRITE(6,*)'INPUT THE SHEAR FORCE F2 (N).'
      READ *,F2
      WRITE(6,*)'INPUT THE NORMAL FORCE F3 (N).'
      READ *,F3
      WRITE(6,*)'INPUT THE BENDING MOMENT M1 (N*mm).'
      READ *,M1
      WRITE(6,*)'INPUT THE BENDING MOMENT M2 (N*mm).'
      READ *,M2
      WRITE(6,*)'INPUT THE TORSIONAL MOMENT M3 (N*mm).'
      READ *,M3
      WRITE(6,*)'INPUT THE NUGGET RADIUS, A (mm).'
      READ *,A
      WRITE(6,*)'INPUT THE SHEET THICKNESS, T (mm).'
      READ *,T
      WRITE(6,*)'INPUT THE MATERIAL CONSTANT (for the Walker eq.), C.'
      READ *,C
      WRITE(6,*)'INPUT THE MATERIAL CONSTANT (for the Walker eq.), m.'
      READ *,M
      WRITE(6,*)'INPUT THE MATERIAL CONSTANT (for the Walker eq.), g.'
      READ *,G
      WRITE(6,*)'INPUT THE LOAD RATIO, R.'
      READ *,R
      WRITE(6,*)'INPUT THE ANGULAR POSTION OF FAILURE, F (rad).'
      READ *, F
      WRITE(6,*)'INPUT THE THRESHOLD STRESS INTESITY FACTOR, BELOW WHICH
     $ NO CRACK WILL GROW.'
      READ *, KTH

******* CALCULATION OF ORIGINAL STRESS INTENSITIES  ****************
      C1=A**(-1.5)
      C2=0.341*((2.0*A/T)**0.397)
      C3=0.282 + 0.162*((2.0*A/T)**0.71)

      K1=C1*(C2*(F1*COS(F)+F2*SIN(F)))
      K1=K1 + 0.282*C1*F3 + 0.846*C1*(M1*SIN(F)-M2*COS(F))/A

      K2=C1*C3*(F1*COS(F)+F2*SIN(F))

      K3=C1*C3*(F1*SIN(F)+F2*SIN(F))

******* ESTIMATE OF THE ANGLE OF CRACK PROPAGATION  ****************
**** THIS ROUTINE USES THE NEWTON-RAPHSON METHOD.  DIFFERENT INITIAL *
```

```
**** GUESSES, TH, WILL EFFECT CONVERGENCE. ************************

    TH=-0.7

    DO 10 I=1,100
     TE=TH - 0.5*(K1*SIN(TH)+3*K2*COS(TH)-K2)/(K1*COS(TH)-K2*SIN(TH))
     IF ((ABS(TE-TH)).LT.(0.001)) THEN
      GOTO 20
     END IF
     TH=TE
10   CONTINUE
20   WRITE(6,*)

******* CALCULATION OF THE EFFECTIVE STRESS INTENSITY FACTOR RANGE ****

    KE=.25*K1*(3*COS(TH/2)+COS(3*TH/2))-.75*K2*(SIN(TH/2)+SIN(3*TH/2))
    KE=KE*(1-R)

*******  LIFE ESTIMATION  ****************************************

    DUM=SQRT(0.001)

    N=C*( (KE*DUM/((1-R)**(1-G)))**(M) )
    NF=-T/(N*SIN(TH))

*******  OUTPUT OF INFORMATION  **********************************

    WRITE(6,*)'Effective SIF Range (Mpa*sqrt(m)) =',KE*DUM*(1-R)
    WRITE(6,*)
    WRITE(6,*)'Effective zero-to-max SIF range =',KE*DUM/((1-R)**(-G))
    WRITE(6,*)
    IF (KE.LT.KTH) THEN
     WRITE(6,*)'STRESS INTENSITY TO SMALL TO GROW A CRACK TO FAILURE.'
    ELSE
    WRITE(6,*)'THETA =',TH
    WRITE(6,*)
    WRITE(6,*) 'Cycles to failure =',NF
    END IF
    END
```

The second program corresponds to the method of Section 2.2. The Secant method is used to solve Eq. 2.13 for Θ_o. This method was chosen because a derivative of Eq. 2.13 is not easily calculated. Although it converges slower than the Newton-Raphson method, its convergence is less dependent on initial values, of which the Secant method needs two instead of one. Values of 1.0 and 0.2 radians seem to work well for the geometries used in this paper. With the exception of calculating Θ_o, this method, and its corresponding program is identical to that of Section 2.1 and its program.

```
   PROGRAM MINLIFE

   REAL   F1,F2,F3,M1,M2,M3,A,T,C,M,G,R,F,TH,KE,NF,C1,C2,C3,DUM,N
   REAL   OLDN,OLDD,NOWN,NOWD,OLD,NOW,TO,TN,K1,K2,K3,KTH
   INTEGER I

******* INPUT OF LOADING, MATERIAL, AND GEOMETRIC INFORMATION *****

   WRITE(6,*)'   CONSTANT GROWTH / NO RESIDUAL STRESS'
   WRITE(6,*)'         LIFE PREDICTION MODEL  '
   WRITE(6,*)
   WRITE(6,*)
   WRITE(6,*)'THIS PROGRAM ESTIMATES THE LIFE OF A SPOT-WELDED'
   WRITE(6,*)'CONNECTION BETWEEN TWO SHEETS OF STEEL.'
   WRITE(6,*)'THE ASSUMPTIONS MADE IN DEVELOPING THIS MODEL ARE'
   WRITE(6,*)'   1. NEGLIGIBLE RESIDUAL STRESSES'
   WRITE(6,*)'   2. CONSTANT MATERIAL PROPERTIES AT CRACK TIP'
   WRITE(6,*)'   3. FORCE AND MOMENT RESULTANTS ARE KNOWN'
   WRITE(6,*)'   4. FORCE AND MOMENT LOAD RATIOS ARE IDENTICAL'
   WRITE(6,*)'      AND CONSTANT'
   WRITE(6,*)'   5. CRACK GROWTH IS CONSTANT'
   WRITE(6,*)'   6. CRACK GROWS SUCH THAT LIFE IS MINIMIZED'
   WRITE(6,*)'   7. ANGLE OF CRACK GROWTH IS CONSTANT'
   WRITE(6,*)'   8. EFFECTIVE STRESS INTENSITY IS RELATED TO'
   WRITE(6,*)'      THE ORIGINAL STRESS INTENSITIES'
   WRITE(6,*)'   9. CRACK REORIENTATION OCCURS AT THE MOMENT'
   WRITE(6,*)'      LOADING BEGINS.'
   WRITE(6,*)'  10. A THRESHOLD VALUE FOR STRESS INTESSITY FACTORS'
   WRITE(6,*)'      EXISTS BELOW WHICH CRACKS DO NOT PROPAGATE.'
   WRITE(6,*)
   WRITE(6,*)
   WRITE(6,*)'SEE FIGURES 1.1 AND 1.2 TO INPUT THE FOLLOWING DATA'
   WRITE(6,*)

   WRITE(6,*)'INPUT THE SHEAR FORCE F1 (N).'
   READ *,F1
   WRITE(6,*)'INPUT THE SHEAR FORCE F2 (N).'
   READ *,F2
   WRITE(6,*)'INPUT THE NORMAL FORCE F3 (N).'
   READ *,F3
```

```
      WRITE(6,*)'INPUT THE BENDING MOMENT M1 (N*mm).'
      READ *,M1
      WRITE(6,*)'INPUT THE BENDING MOMENT M2 (N*mm).'
      READ *,M2
      WRITE(6,*)'INPUT THE TORSIONAL MOMENT M3 (N*mm).'
      READ *,M3
      WRITE(6,*)'INPUT THE NUGGET RADIUS, A (mm).'
      READ *,A
      WRITE(6,*)'INPUT THE SHEET THICKNESS, T (mm).'
      READ *,T
      WRITE(6,*)'INPUT THE MATERIAL CONSTANT (for the Walker eq.), C.'
      READ *,C
      WRITE(6,*)'INPUT THE MATERIAL CONSTANT (for the Walker eq.), m.'
      READ *,M
      WRITE(6,*)'INPUT THE MATERIAL CONSTANT (for the Walker eq.), g.'
      READ *,G
      WRITE(6,*)'INPUT THE LOAD RATIO, R.'
      READ *,R
      WRITE(6,*)'INPUT THE ANGULAR POSTION OF FAILURE, F (rad).'
      READ *, F
      WRITE(6,*)'INPUT THE THRESHOLD STRESS INTESITY FACTOR, BELOW WHICH
     $  NO CRACK WILL GROW.'
      READ *, KTH

******* CALCULATION OF ORIGINAL STRESS INTENSITIES *****************
      C1=A**(-1.5)
      C2=0.341*((2.0*A/T)**0.397)
      C3=0.282 + 0.162*((2.0*A/T)**0.71)

      K1=C1*(C2*(F1*COS(F)+F2*SIN(F)))
      K1=K1 + 0.282*C1*F3 + 0.846*C1*(M1*SIN(F)-M2*COS(F))/A

      K2=C1*C3*(F1*COS(F)+F2*SIN(F))

      K3=C1*C3*(F1*SIN(F)+F2*SIN(F))

******* ESTIMATE OF THE ANGLE OF CRACK PROPAGATION  *****************
**** THIS ROUTINE USES THE SECANT METHOD.  DIFFERENT FIRST CHOICES ***
**** WILL EFFECT CONVERGENCE.  ************************************

      TN=-1.0
      TO=-0.2

      DO 10 I=1,100

      OLDN=K1*(SIN(.5*TO)+SIN(1.5*TO))+K2*(COS(.5*TO)+3*COS(1.5*TO))
      OLDD=K1*(3*COS(.5*TO)+COS(1.5*TO))-3*K2*(SIN(.5*TO)+SIN(1.5*TO))
       OLD=TAN(TO)*(OLDN/OLDD)-(2.0/(3.0*M))

      NOWN=K1*(SIN(.5*TN)+SIN(1.5*TN))+K2*(COS(.5*TN)+3*COS(1.5*TN))
      NOWD=K1*(3*COS(.5*TN)+COS(1.5*TN))-3*K2*(SIN(.5*TN)+SIN(1.5*TN))
```

```
      NOW=TAN(TN)*(NOWN/NOWD)-(2.0/(3.0*M))
      IF ((ABS(OLD-NOW)).LT.(0.0001)) THEN
       GOTO 20
      END IF
       TH=TN
       TN=TN+(TN-TO)*(NOW/(OLD-NOW))
       TO=TH

10    CONTINUE
20        WRITE(6,*)


******* CALCULATION OF THE EFFECTIVE STRESS INTENSITY FACTOR  ***********
***** THE MODE II STRESS INTENSITY FACTOR IN THIS DIRECTION OF GROWTH ***
***** IS ASSUMED TO HAVE NO CONTRIBUTION TO THE EFFECTIVE S.I.F. ********

     KE=.25*K1*(3*COS(TH/2)+COS(3*TH/2))-.75*K2*(SIN(TH/2)+SIN(3*TH/2))
     KE=KE*(1-R)

*******  LIFE ESTIMATION  ****************************************

     DUM=SQRT(0.001)

     N=C*( (KE*DUM/((1-R)**(1-G)))**(M) )
     NF=-T/(N*SIN(TH))

*******  OUTPUT OF INFORMATION  **********************************

     WRITE(6,*)'Effective SIF Range (Mpa*sqrt(m)) =',KE*DUM*(1-R)
     WRITE(6,*)
     WRITE(6,*)'Effective zero-to-max SIF range =',KE*DUM/((1-R)**(-G))
     WRITE(6,*)
     IF (KE.LT.KTH) THEN
      WRITE(6,*)'STRESS INTENSITY TO SMALL TO GROW A CRACK TO FAILURE.'
     ELSE
     WRITE(6,*)'THETA =',TH
     WRITE(6,*)
     WRITE(6,*) 'Cycles to failure =',NF
     END IF
     END
```

TABLE B.1 - SPOT-WELD LOADS FOR VARIOUS SPECIMEN GEOMETRIES
(See Figure 1.1 for details of applied loads and moments)

GEOMETRY	F1 (shear force)	F2 (shear force)	F3 (normal force)	M1 (bending)	M2 (bending)	M3 (torsion)
Lap joint	P	0	0	0	0	0
Peel joint (original)	0	0	P	0	20mm x -P	0
Peel joint (modified)	0.707 x P	0	0.707 x P	0	14mm x -P	0
Box joint (bending only)	1.9974 x P	0	0	0	0.540mm x-P	0
Box joint (bending and torsion)	2.604 x P	0	0	0	0.73mm x-P	0

TABLE B.2 - VARIABLES AND CONSTANTS USED

Quantity	Value
Stress Intensity Threshold, Kth	0
weld radius, a	3.5 mm
sheet thickness, t	1.0 mm
Walker Eqn. constant, C	1.00E-09
Walker Eqn. constant, m	3
Walker Eqn. constant, gamma	0.5

It should be noted that the units of all quantities listed in Table B.1 are given in SI units. This is so because the FORTRAN codes were written to handle those units. Since the load-life plots given in Chapter 3 are shown with US units this may create some confusion

VITA

Since birth on February 24, 1971 in Newport News, Virginia, John Andrew "Andy" Newman has lived in Virginia his entire life. Education has always been important in his life, due in part to both parents being educators. After living in Hampton, Virginia for 18 years he graduated from Kecoughtan High School in 1989. Hobbies for Andy include hiking, auto repair, hunting, shooting, camping, rock climbing, and occasionally studying. Virginia Tech was chosen for higher education because of Tech's solid engineering program and its semi-rural location. After a shaky start in college Andy finally graduated from Tech in 1994 with a bachelor's degree in Engineering Science and Mechanics. Graduation with a master's degree is expected in early fall of 1996. He married Lisa Earlene Hitt on May 18, 1996. Future plans are not solid at this point, but pursuit of a doctorate degree in Engineering Mechanics is a strong possibility.

John Andrew Newman